MODELING OF BIPEDAL ROBOT
NEGOTIATING SLOPES

A dissertation submitted to the

Department of Electrical Engineering, University of Moratuwa

in partial fulfilment of the requirements for the

Degree of Master of Science

by

M.G.A.P. ABEYRATNE

Supervised by: Prof. Lanka Udawatta

Department of Electrical Engineering

University of Moratuwa

Sri Lanka

2010

94547

Abstract

This research shows how the robotics theories are applied to model the bipedal walking robot. Utilizing the direct kinematics and inverse kinematics, the kinematic model for the robot is developed. The derivation of joint angle equations for 6 links Robot, walking on a slopping surface, is a direct approach in this research. The development of hip trajectory is another important invention specific to this research.

The dynamic stability is analyzed by utilizing ZMP criteria. The calculation of ZMP for this model is very complex and based on mechanics theories. The selection of iteration method to calculate linear accelerations of each link (which are used to calculate ZMP) is guaranteed by simulation results.

The dynamic stability is analyzed for lower body using ZMP simulation results. For this case the "Dynamic" Balance Margin (DBM) is introduced and requirement for stability is also introduced.

The methods or precautions that can be used to improve ZMP are identified. The most effected method for improve the stability is selected as control of torso angle. Finally, the modified ZMP is re-derived with the term of torso angle and it is found that the ZMP can be moved to safe margin by controlling torso angle. The results show the effectiveness of the proposed methodology.

DECLARATION

The work submitted in this dissertation is the result of my own investigation, except where otherwise stated.

It has not already been accepted for any degree, and is also not being concurrently submitted for any other degree.

UOM Verified Signature

Name of Candidate - M.G.A.P. Abeyratne

Date – 8th February 2010

We/I endorse the declaration by the candidate.

UOM Verified Signature

Name of the Supervisor – Prof. Lanka Udawatta

Contents

Acknowledgement

I express my gratitude to my supervisor, Professor Lanka Udawatta, for his great supervision, guidance and support provided to me to do this research. My sincere thanks go to the officers in Post Graduate Office, Faculty of Engineering, University of Moratuwa, Sri Lanka for helping me in various ways to clarify the things related to my academic works in time with excellent assistance. Sincere gratitude is also extended to the people who serve in the Department of Electrical Engineering office for their immense support provided to me.

I extend my sincere appreciation to Dr. Thrishantha Nanayakkara in Kingston College, London for his valuable support and for furnishing new information in the field of biped robot. Also, thanks are due to Mr. S.M. Welihinda, who helped me by simulating the derived model and showing the correctness of the derivations.

An especial thank is due to my spouse, Mrs. H.M.S.N. Kularatne, for providing utmost support in preparing this dissertation properly.

Sincere thanks are due to many individuals, friends and colleagues who helped me in various ways to complete this project. May be I would not be able to made it without the support of you all.

List of Figures

List of Tables

Chapter 1

Introduction

1.1   General introduction to robotics

Robotics has achieved its greatest success to date in the world of manufacturing industry. Robot arms, or manipulators, comprise a 2 billion dollar industry. Bolted at its shoulder to a specific position in the assembly line, the robot arm can move with great speed and accuracy to perform repetitive tasks such as spot welding and painting (Figure 1.1) [1]. In the industry of electronics, manipulators place surface-mounted components with superhuman precision, making the portable telephone and laptop computer possible.
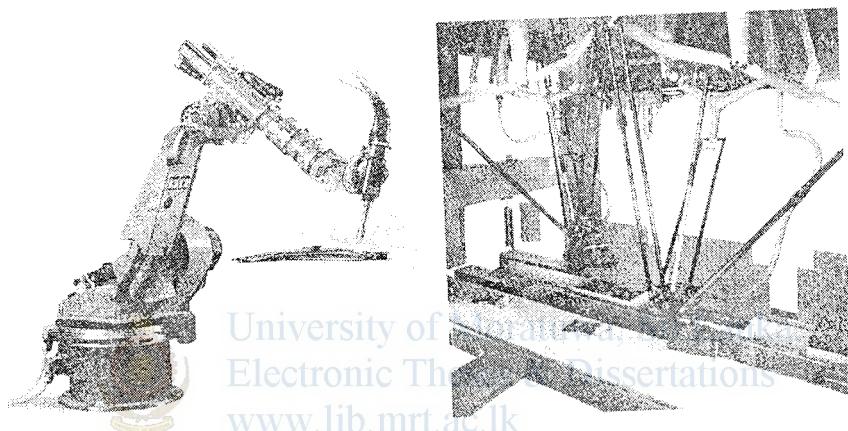
Figure 1.1: Picture of auto assembly plant –spot welding robot of KUKA

To sum up, machines that can replace human beings as regards to physical work and decision making are categorized as *robots* and their study as *robotics*. The robot technology is advancing rapidly. The industry is moving from the current state of automation of robotization, to increase productivity and to deliver uniform quality. Robots and robot-like manipulators are now commonly employed in hostile environment, such as at various places in an atomic plant for handling radioactive materials. Robots are being employed construct and repair space stations and satellites. There are now increasing number of applications of robots such as in nursing and aiding a patient. Micro robots are being designed to do damage control inside human veins. Robot like systems are now employed in heavy earth-moving equipment. It is not possible to put up an exhaustive list of robot applications. One type of robot commonly used in the industry is a robotic manipulator or simply a *manipulator* or a *robotic arm*. It is an open or closed kinematic chain of rigid links interconnected by movable joints. In some configurations, links can be considered to correspond to human anatomy as waist, upper arm, and forearm with joints at shoulder and elbow. At the end of the arm, a wrist joint connects and *end-effector* to the forearm. The end-effector may be a tool and its fixture or a *gripper* or any other device to do the work.

The end-effector is similar to the human hand with or without fingers. A robotic arm, as described above is shown in figure 1.2, where various joint movements are also indicated.
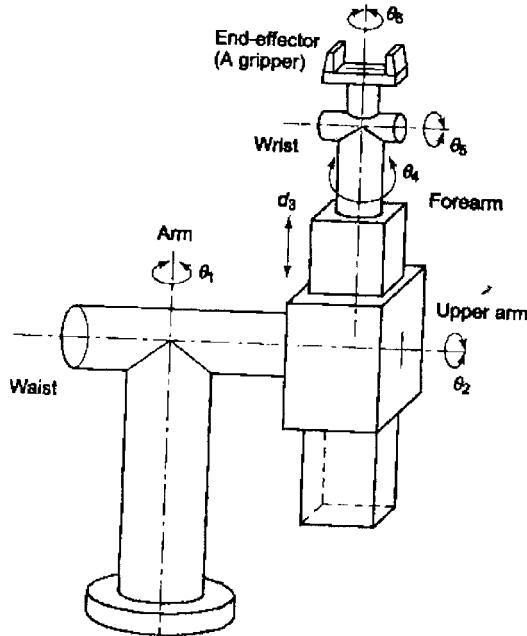
Figure 1.2: An industrial robot that least looks like a human

1.1.1 What is and what is not a robot

Automation as a technology is concerned with the use of mechanical, electrical, electronic, and computer-based control systems to replace human beings with machines, both for physical work and the process of intelligent information processing. Industrial automation, which started in the eighteenth century as fixed automation has transformed into flexible and programmable automation in the last 15 or 20 years. Computer Numerically Controlled (CNC) machine tools, transfer, and assembly lines are some examples in this category.

Common people are easily influenced by science fiction and thus, imagine a robot as a humanoid that can walk, see, hear, speak, and do the desired work. But the scientific interpretation of science fiction scenario propounds a robot as an automatic machine that is able to interact with and modify the environment in which it operates. Therefore, it is essential to define what constitutes a robot. Different definitions from diverse sources are available for a robot.

Japan is the world leader in robotics development and robot use. Japan Industrial Robot Association (JIRA) and the Japanese Industrial Standards Committee defines the industrial robot at various levels as:

2

Manipulator: a machine that has functions similar to human upper limbs, and moves the object spatially.

Playback robot: a manipulator that is able to perform an operation by reading off the memorized information for an operating sequence, which is learned beforehand.

Intelligent Robot: a robot that can determine its own behavior and conduct through its functions of sense recognition.

The British Robot Association (BRA) has defined the industrial robot as:

"A reprogrammable device with minimum of four degrees of freedom designed to both manipulate and transport parts, tools, or specialized manufacturing implements through variable programmed motions for performance of specific manufacturing task."

The Robotics Industries Association (RIA)of USA defines the robot as:

"A reprogrammable, malfunctioned, manipulator designed to move material through variable programmed motions for the performance of a variety of tasks"

The definition adopted by Internal Standards Organization (ISO) and agreed upon by most of the users and manufactures is:

"An industrial robot is an automatic, servo-controlled, freely programmable, multipurpose manipulator, with several areas, for the handling of work pieces, tools, or special devices. Variably programmed operations make the execution of a multiplicity o tasks possible".
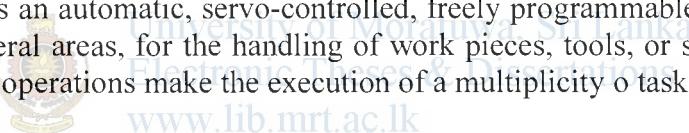
Although there is a wide range of definitions exist, none covers the features of a robot comprehensively. The RIA definition lays importance on programmability, while the BRA definition succeeds minimum degrees of freedom. The JIRA definition is fragmented. As a result of these, still it is uncertain in distinguishing a robot from automation and in describing functions of a robot. To differentiate between a robot and automation, following guidelines can be used.

For a machine to be called a robot, it must be able to respond to stimuli based on the information received from the environment. The robot must interpret the stimuli either passively or through active sensing to bring about the changes required in its environment. The decision-making, performance of tasks and so on, all are done as defined in the programs taught to the robot. The functions of a robot can be classified in to three areas as follows.

"Sensing" the environment by external sensors, for example, vision, voice, touch, and proximity and so on, "decision-making" based on the information received from the sensors, and "performing" the task decided.

3

1.1.2 Laws of Robotics

Issac Asimov conceived the robots as humanoids, devoid of feelings, and used tem in a number of stories. His robots were well-designed, fail-safe machines, whose brains were programmed by human beings. Anticipating the dangers and havoc such a device could cause, he postulated rules for their ethical conduct. Robots were required to perform according to three principles known as "three laws of robotics", which are as valid for real robots as they were for Asimov's robots, and they are:

1. A robot should not injure a human being or, through inaction, allow a human to be harmed.
2. A robot must obey orders given by humans except when that conflicts with the First Law.
3. A robot must protect its own existence unless that conflicts with the First or Second Law.

These are very general laws and apply even to other machines and appliances. They are always taken care of in any robot design.

1.1.3 Robot Anatomy

The mechanical structure of a robot is like the skeleton in the human body. Therefore the robot anatomy is studying of the robot skeleton that means the physical construction of the manipulator structure.
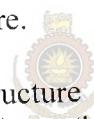
The mechanical structure of a manipulator consists of rigid bodies (links) connected by means of articulations (joints), is segmented into an arm that ensures mobility and reachability, a wrist that confers orientation, and an end effector that performs the required task. Most manipulators are mounted on a base fastened to the floor or on the mobile platform of an autonomous guided vehicle (AGV). The arrangement of base, arm, wrist, and end-effector is shown in figure 1.3.
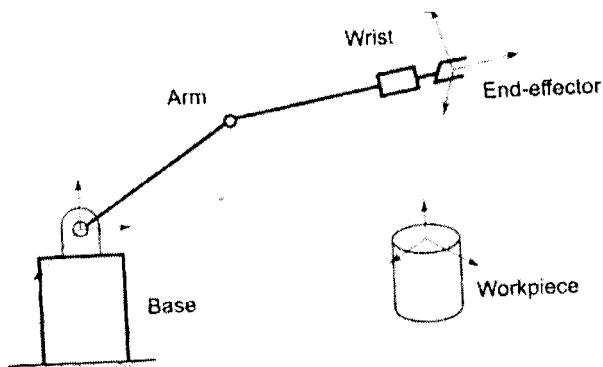
Figure 1.3: The base, arm, wrist, and end-effector forming the mechanical structure of a manipulator

1.1.4   Robot applications

Robotics has rapidly moved from theory to applications and from the research labs to industries over the last 20 years or so years. The mathematical models developed help in design of robots, calculating their motions, control them and plan or determine the trajectory and frame transformations required for performing specified tasks during the work cycle.

One of the key features of a robot is its versatility. As a designer, developer, planner or user of this technology one has to be familiar with the various issues involved in the applications of robots. As the technology is new, the prospective user or buyer of robot technology, who is accustomed to buy conventional items, will find the robot applications a complex subject.

The industrial application of robotics is going to be a prominent component of manufacturing industry, which will affect human labour at all levels, from managers of production to shop floor unskilled workers. A programmable robot with a number of degrees of freedom and different configurations can perform specific and diverse tasks with the help of the variety of end-effectors. On the industrial scene it can be reprogrammed and adapted to changes in process or production line. Robots are also finding many applications outside of the industry, in research, hospitals, space, supermarkets, service sector, farmhouses, and even in homes as pets. The applications outside of a factory are much more complex, diverse and are based on human imagination.

When talking about robot applications in industry as well as other places, one needs to be concerned about the safety. After all, a robot, as it is today and going to be for decades to come, is a dumb machine, which is supposed to obey the commands.

Although robots are becoming common in the workplace, it is important to remember that robots are not "super workers". They have some real shortcomings and are to be understood as tools or machine people use.

Today's robots:

- Are not creative or innovative
- Can not react to unknown situations
- Have no human feelings
- Have not consciousness
- Do not think independently
- Can not make complicated decisions.
- Do not learn from mistakes or otherwise.
- Do not adapt quickly to the changes in their environment.

The current day applications of robots can be categorized into two broad areas: industrial applications and non industrial applications.

Of the robots in the world today about 90% are found in industries. These robots are referred to as industrial robots and are regarded as "Steel Coller Workers". Of these more than 50% are deployed in automotive industry. Robots are useful in the industries in many ways. In today's economy, industry needs to be efficient to cope with the competition. Installing robots in the industry is often a step to be more competitive because robots can do certain tasks more efficiently than humans.

Some of the tasks Robots can do better are:
- Handling dangerous materials
- Assembling products
- Spray finishing
- Polishing and cutting
- Inspection
- Repetitive, backbreaking and unrewarding tasks
- Tasks involving dangerous to humans or dangerous tasks

Robots offer and excellent means of utilizing technology to make a given manufacturing operation more profitable and competitive. The main advantage offered for the industrial needs is the improved productivity and quality offered by the robots. However, the technology is relatively new on the industrial scene. Its use in the manufacturing processes is greatly limited for multiple reasons.

Robots applications in the industries today are primarily in four fields:
- Material handling
- Operations
- Assembly
- Inspection

1.2 Robot locomotion

A mobile robot needs locomotion mechanisms that enable it to move unbounded throughout its environment. But there are a large variety of possible ways to move, and so the selection of robot's approach to locomotion is an important aspect of mobile robot design. In the laboratory, there are research robots that can walk, jump, run, slide, skate, swim, fly and, of course, roll. Most of these locomotion mechanisms have been inspired by their biological counterparts.

There is, however, one exception: the actively powered wheel is a human invention that achieves extremely high efficiency on flat ground. This mechanism is not completely foreign to biological systems. Our bipedal walking system can be approximated by a rolling polygon, with sides equal in length d to the span of the step (Figure 1.4) As the step size decreases, the polygon approaches a circle or wheel. But nature did not develop a fully rotating, actively powered joint, which is the technology necessary for wheeled locomotion.
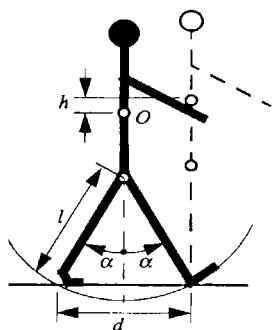
Figure 1.4: Approximated bipedal walking system

Biological systems succeed in moving through a wide variety of harsh environments, Therefore it can be desirable to copy their selection of locomotion mechanisms. However, replicating nature in this regard is extremely difficult for several reasons. To begin with, mechanical complexity is easily achieved in biological systems through structural replication. Cell division, in combination with specialization can readily produce a millipede with several hundred legs and several tens of thousands of individually sensed cilia. In man made structures, each part must be fabricated individually and so no such economies of scale exit. Additionally, the cell is a microscopic building block that enables extreme miniaturization. With very small size and weight, insects achieve a level of robustness that we have not been able to match with human fabrication techniques. Finally, the biological energy storage system and the muscular and hydraulic activation systems used by large animals and insects achieve torque, response time, and conversion efficiencies that far exceed similarly scaled man-made systems.

Owing to these limitations, mobile robots generally locomote either using wheeled mechanisms, a well-known human technology for vehicles, or using a small number of articulated legs, the simplest of the biological approaches to locomotion (Figure 1.4).

In general, legged locomotion requires higher degrees of freedom and therefore greater mechanical complexity than wheeled locomotion. Wheels, in addition to being simple, are extremely well suited to flat ground. On flat surfaces wheeled locomotion is one to two orders of magnitude more efficient than legged locomotion. The railway is engineered for wheeled locomotion because rolling friction is minimized on a hard and flat steel surface. But, as the surface becomes soft, wheeled locomotion accumulates inefficiencies due to rolling friction whereas legged locomotion suffers much les because it consists only of points contacts with the ground.

In effect, the efficiency of wheeled locomotion depends greatly on environmental qualities, particularly the flatness and hardness of the ground, while the efficiency of legged locomotion depends on the leg mass and body mass, both of which the robot must support at various points in a legged gait.

1.2.1 Key issues for locomotion

Locomotion is the complement of manipulation. In manipulation, the robot arm is fixed but moves objects in the workspace by imparting force to them. In locomotion, the environment is fixed and the robot moves by imparting force to the environment. In both cases, the scientific basis is the study of actuators that generate interaction forces, and mechanisms that implement desired kinematic and dynamic properties. Locomotion and manipulation thus share the same core issues of stability, contact characteristics, and environment type:

- Stability

  1. Number and geometry of contact points
  2. Centre of gravity
  3. Static/dynamic stability
  4. Inclination of terrain

- Characteristics of contact

  1. Contact point/path size and shape
  2. Angle of contact
  3. Friction

- Type of environment

  1. Structure
  2. Medium (eg. Air, water etc..)

A theoretical analysis of locomotion begins with mechanics and physics. From this starting point, we can formally define and analyze all a manner of mobile robot locomotion systems.

1.3 Legged Mobile Robot

Legged locomotion is characterized by a series of point contacts between the robot and the ground. The key advantages include adaptability and maneuverability in rough terrain. Because only a set of point contacts is required, the quality of the ground between those points does not matter so long as the robot can maintain adequate ground clearance. In addition, a walking robot is capable of crossing a hole or chasm so long as its reach exceeds the width of the hole. A final advantage of legged locomotion is the potential to manipulate objects in the environment with great skill.

The main disadvantages of legged locomotion include power and mechanical complexity. The leg, which may include several degrees of freedom, must be capable of sustaining part of the robot's total weight, and in many robots must be capable of lifting and lowering the robot. Additionally, high maneuverability will only be achieved if the legs have a sufficient number of degrees of freedom to impart forces in number of different directions.

1.3.1 Leg configuration and stability

Legged robots are biologically inspired and therefore, it is informative to examine biologically successful legged systems. A number of different leg configurations have been successful in a variety of organism. Large animals have four legs, where as insects have six or more legs. In some mammals, the ability to walk on only two legs have been perfected.

1.3.2 Biped Robot

Out of various designs of multi legged robots, two legged robots have received much attention in robotics research, due to their similarity with the human beings. A gait is a sequence of leg motions coordinated with the body motion for the purpose of navigating over a terrain. It is important to mention that a two legged robot has to dynamically balance during its locomotion.

A biped robot should be able to negotiate the stair-cases sloping surfaces, ditches and others, as the situation demands. The problems of tackling the sloping surface[2] is fundamentally different form that of handling the stair-cases due to the following reasons:

- The feet are places on the inclined plane while navigating along a sloping surface, in place of the flat surface.
- The angle of slope and coefficient of friction between the sloping surface and foot has some significant influences to ensure the movement without slipping on an inclined plane.
- The projected area of foot-support polygon reduces with the increase in angle of slope and it has a significant contribution on the dynamic balance of the robot.

1.3.3 Biped walking

In order to understand the mechanical bipedal robots mechanics design[3], is necessary first to understand the biped walking process or biped locomotion. This area has been studies for a long time, but, it is only in the past years, thanks to the fast development of computers, that real robot started to walk on two legs. Since then the problem has been tackled from different directions.

First, there were robots that used static walking. The control architecture had to make sure that the projection of the centre of gravity on the ground was always inside the foot support area. This approach was abandoned because only slow walking speeds could be achieved, and only on flat surfaces.

Then dynamic walking robots appeared, the center of gravity (or centre of mass) can be outside of the support are, but the Zero Momentum Point (ZMP), which is the point where the total angular momentum is zero, cannot. Dynamic walkers can achieve faster walking speeds, running, star climbing, execution of successive flips, and even walking with no actuators.

Static walking: Static walking assumes that the robot is statically stable. This mean that, at any time if all motion is stopped the robot will stay indefinitely in a stable position. It is necessary that the projection of the centre of gravity of the robot on the ground must be contained within the foot support area (Figure 1.5). The support area is either the foot surface in case of one supporting leg minimum convex area containing both foot surfaces in case both feet are on the ground. These are referred to as single and double support phases, respectively. Also, walking speed must be low so that inertial forces are negligible.

This kind of walking requires large feet; strong ankle joints and can achieve only slow walking speeds. It has been abandoned by most researches for dynamic walking, which provides more realistic and agile movements.
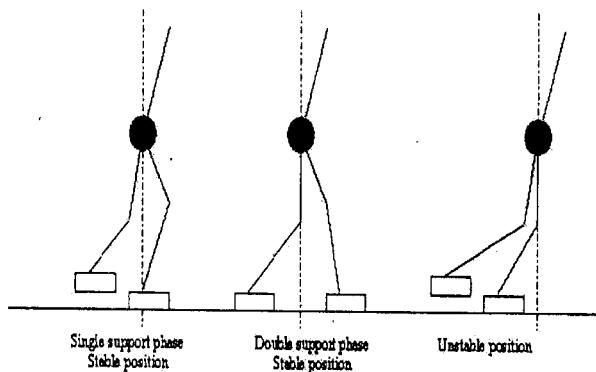
Figure 1.5: Stability in static walking

Dynamic walking: Biped dynamic walking allows the centre of gravity to be outside the support region for limited amounts of time. There is no absolute criterion that determines whether the dynamic walking is stable or not. Indeed a walker can be designed to recover from different kinds of instabilities. However, if the robot has active ankle joints and always keeps at least one foot flat on the ground then the ZMP can be used as a stability criterion. The ZMP is the point where the robot's total moment at the ground is zero. As long the ZMP is inside the support region the walking is considered dynamically stable because is the only case where the foot can control the robot's posture. It is clear that for robots that do not continuously keep at least one foot on the ground or that do not have active ankle joints (walking on stilts), the notion of support area does not exist, therefore the ZMP criterion cannot applied.

Dynamic walking is achieved by ensuring that the robot is always rotating around a point in the support region. If the robot rotates around a point outside the support region then this means that the supporting foot will tend to get off the ground or get presses against the ground. Both cases lead to instability. To draw an analogy with static walking, if all motion is stopped then the robot will tend to rotate around the ZMP.

1.4   Research objectives

The main objective of this research is to implement a kinematic model for biped robot to negotiate sloping surfaces. The derivation of equations for joint angles of the said robot is the kinematc modeling. In this research, the basic robotics theories are used to implement the kinematic model and it is a direct approach. This research can be divided into two steps as follows;

     (i)   Development of kinematic model
     (ii)   Simulation and behavioral analysis

After developing the kinematic model, the behavioral analysis can be obtained by using the simulation result. The stability analysis is so important to select parameters, in the construction stage, of the robot body.

In this dissertation, it is considered only walking on sagital plane and assumed all joints are frictionless. This is a remarkable modeling as the robot can maintain it's stability with no trouble when increasing the ramp angle to some extent. The modeling method is simple, direct and inexpensive but, the accuracy is in high standard that can be seen in simulation results.

1.5   Overview

The structure of this dissertation divided in to 8 parts. Chapter 2, reviews past literature and the current state of research in bipedal robots. Also, the Problem Statement is included. In chapter 3, kinematic modeling of swing leg is included and derivations of equations for joint angles are also presented. In chapter 4, the gait development is discussed with trajectory planning of swing leg. Chapter 5, describes, how to obtain the kinematic model of stance leg. In this chapter joint angle equations are also derived and, the derived swing leg kinematic model is modified by considering "moving hip". To model the hip trajectory the Rimless wheel simulation is used. In chapter 6, it is discussed how to analyze the dynamic balance for lower body and calculation of ZMP. The chapter 7 describes the calculation of ZMP after adding of torso. In this chapter the simulation results and explanations are included. Chapter 8 concludes all derivations and presented the future work of this research.

Chapter 2

Literature Review and Problem Statement

2.1   Literature Review

The first biped robot to be successfully created and use dynamic balance was developed by Kato in 1983 [4]. While this robot largely used static walking, it was termed quasi-dynamic due to a small period in the gait where the body was tipped forward to enable the robot to gain forward acceleration and thus achieve a forward velocity. This achievement has largely been cited as the defining moment where the focus of research shifted from static to dynamic walking.

Since this time, progress has been somewhat sluggish. The same research group produced the WL-10RD robot which walked once more with quasi-dynamic balance in 1985[5]. The robot was required to return again to static balance after the dynamic transfer of support to the opposite foot. However, Miura and Shimoyama [6] abandoned static balance entirely in 1984 when their stilt biped BIPER-3, which was modeled after a human walking on stilts, showed true active balance. Simple in concept, it contained only three actuators; one to change the angle separating the legs in the direction of motion, and the remaining two which lifted the legs out to the side in the lateral plane. Since the legs could not change length, the slide actuators were used to swing the leg through without scuffing the foot on the walking surface. An inverted pendulum was used to plan for foot placement by accounting for the accelerating tipping moments which would be produced. This three degree-of-freedom robot was later extended to the seven degree-of-freedom BIPER-4 robot.

Another approach had been taken by Raibert[7], who developed a planer hopping robot. This robot used a pneumatically driven leg or the hopping motion and was attached to a tether which restricted the motion to three degrees of freedom (pitch motion, vertical and horizontal translation) along a radial path inscribed by the tether. A state machine was used to track the current progress of the hopping cycle, triggered by sensor feedback. The state machine was then used to modify the control algorithm used to ensure the stability of the machine. A relatively simple control system was used which modified three parameters of the hopping gait, namely forward speed, foot placement and body attitude. The success of this research motivated Raibert to extend the robot and control system to hopping in three dimensions, pioneering the area of ballistic flight in legged locomotion.

Continuing through the years, a dynamic running robot was developed by Hodgins, Koechling and Raibert [7],[8], extending the previous studies of one-legged hopping machines in two and three dimensions. This robot was constrained to two dimensions

12

(motion in the sagittal plane), and used a similar control method as for the hopping robot in two dimensions. This control system decoupled the three important control parameters of body height, foot placement and body attitude, controlling these three aspects of the running gait through the use of a state machine. The state machine switched states when certain key feedback events occurred, and the robot was controlled differently depending upon the current state of the system.

Much early research around this time focused on intensely analytical techniques for designing and controlling robot motion. This had the tendency to produce complex equations governing the motion of the robot, which often had no solution and had to be approximated or linearised. Sometimes this approach was successful despite such shortcomings. Kajita *et al* [9] used this approach to control bipedal dynamic walking by restricting the movement of the centre of mass (COM) in an ideal sense to the horizontal plane only. This motion was termed a "potential energy conserving orbit" and could be expressed by a simple linear differential equation, which simplified the calculations involved.

Other similar analytical approaches actually increased the complexity of the problem by introducing new links to the bipedal model. Takanishi *et al.* [10] used the robot WL-12RIII with a control system which manipulated the zero moment point (ZMP) to achieve dynamic stability, even on uneven surfaces. This robot had seven links including a trunk or upper torso link with two degrees of freedom, thus allowing it to pith and roll relative to the forward direction of the robot. As an extension to this work, Yamaguchi *et al.*[11] used the robot WL-12RV in a similar fashion, adding the feature of a yaw-axis movement to the trunk motion. This allowed compensation for yaw moments occurring about the foot in contact with the ground, eliminating the unwanted behaviour of the robot to turn at higher velocities. This addition allowed the robot to travel 50 percent faster than previous efforts had achieved.
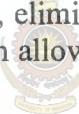
A different analytical approach examined how mechanical design contributes to robot performance. McGeer[12] showed that a correctly designed biped walker with no actuation and no control could walk down gentle slopes. His research showed that passive dynamic walking is possible[1]. The slope allowed the robot to regain through gravity energy lost through friction and impulse collisions. Garcia *et al.* [13] also showed this using the simplest purely mechanical model possible-a double pendulum. This work highlighted the fact that mechanical design is equally, if not more important, than the control method used. This suggests that more effort spent on ensuring a correct mechanical system design will simplify the complexity of the control system required.

A third approach to bipedal dynamic walking has only recently emerged in the last few years. Analysis using the dynamic equations of motion can be complex, non-linear and may have no closed form solution. Artificial neural networks are well suited to this type of control problem having the advantage that they can learn and adopt the behaviour of the system to a desired state, even if this state is not clearly defined. The benefits of this approach is that complex dynamics and kinematic equations need not to be known, or greatly simplified version may be used instead. The result is that neural networks may be

---

[1] The term passive here refers to the fact that actuation is not present in this walker

13

used in real-time to adapt the walking gait on-line, a problem which previous control methods have not been able to significantly address.

Doerschuk *et al.* [14, 15] applied an intelligent learning approach to control the legs of a simulated biped robot while in ballistic flight. They used a Cerebellar Model Articulation Controller (CMAC) neural network to impose a previously generated gait onto a simulated seven link biped robot. A more impressive use of neural networks can be seen in the research of Miller and Kun[16,17], who used three CMAC neural networks in an attempt to produce a control system which could operate in a wider range of environments by adapting various parameters of the walking gait such as step length, step height and step period. One network was used to learn the required motions to achieve side balance in the sagittal plane, one performed forward/backward balance in the lateral plane, and the last network learned the closed chain kinematics in order to keep the feet parallel to the ground via actuated ankles. While not entirely successful, the robot did learn the required behaviour in order to start walking from a stationary position and later come to rest through variation of the parameters within a limited range.

More recent research is being performed in the United Kingdom by the Shadow Robot Group who have developed the Shadow Walker prototype (see figure 2.1). Following an anthropomorphic design and using a wooden frame, they have constructed a biped robot using special 'air' muscles developed by the group. The pneumatic air muscle behaves in a similar manner to a biological muscle, contracting up to 40% of its length when actuated with a supply of air. The complaint muscle has a power to weight ration of approximately 400:1, vastly outperforming conventional actuators. Twenty-eight air muscles(Fourteen per leg) actuate the eight joints in the robot. With twelve degrees of freedom, the muscle arrangement is designed to closely mimic the human leg muscles by placing the air-muscles in corresponding human muscle points.

Another current research project is the WABIAN Humanoid project at the University of Waseda in Japan. The aim of this research group is to develop anthropomorphic robot mechanism using bio-mechatronic techniques. This includes research on human motion dynamics, human-like mechanisms design, and mind analysis and synthesis. Based upon the previous work by Kato, Takanishi and Yamaguchi, with the WL series of robots, the project was established in 1992 to combine the fields of vision, information processing, brain modeling, mechanical design, active sensor integration (tactile, visual and sound), robot psychology, speech recognition and conversation. In an attempt to enable robots and humans to build common mental and physical spaces, the project comprises of over 50 full-time researchers.

14

**Figure 2.1: A photograph of shadow biped robot
(source-http://www.shadow.org.uk/)**
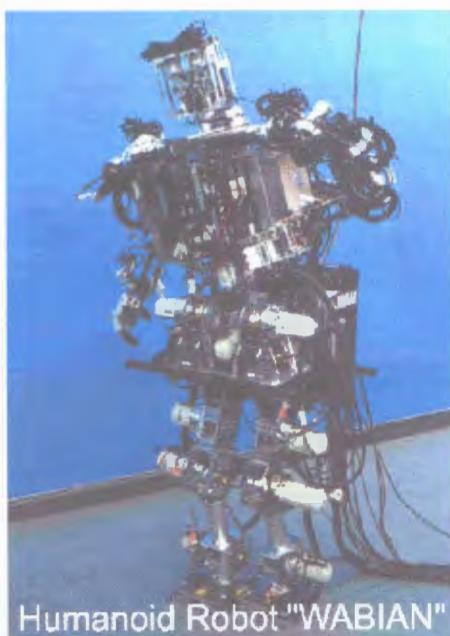
**Figure 2.2: A photograph of wabian robot
(source http://www.shirai.info.waseda.ac.jp)**

2.2 Problem Statement

In this chapter, the necessity of this research is discussed and the dissimilarity from the other related researches is justified. A direct method to stabilize the robot, when it looses the stability, is one of the new and remarkable findings of this work. These contents are described under the following three sub topics.

2.2.1 Preliminaries

Most of the previous works in this field have focused on derivation of kinematics with the use of Artificial Intelligence. Vundavilli and Pratihar [2] have proposed a method for swing leg kinematics by using a neural network. It is not a direct application of robotics technology theories. The major difficulty of this method is building of neural network as it needs large number of data for training, called training cases. The accuracy of this method depends on the number of training cases used to train the neural network. Yamaguchi, Takanashi and Kato [11] have used trunk swing and yaw motions to increase the locomotion stability of a robot. This approach has applied only for walking on a flat surface. Agrawall [24] has proposed a method to identify joint motion of BIPED robots and derived the mathematical model but, has not solved the equations due to its complexity. Zerrugh and Radeliffe [25] have investigated the walking pattern for a BIPED robot by recording human kinematics data. This concept has been deeply studied and understood that it is very difficult to apply these data to practical BIPED robots. Because, the human leg consists of large number of degree of freedoms and having complex joints.

2.2.2 Problem Identification

When consider the previous work done in Bipedal walking we can identify that the latest topic as ramp walking. The latest developed robot Asimo can negotiate staircases only. It can not negotiate inclined surfaces as its legs have been designed for vertical and horizontal movements only. In ramp walking, stability is a problem than in staircase handling because, in ramp walking, the stance foot is in inclined surface and it touches the flat surface in staircase handling. By focusing with previous papers, it is noted that a limited papers were published in this field and no direct approach to derivation of kinematic model. Also it has not introduced a direct method in previous research studies to re-stabilize the robot if it is in an unstable zone.

2.2.3 New suggestions

In this dissertation the derivation of kinematic model, i.e. derivation of joint angle equations, is based on direct kinematics and inverse kinematics. Link transformation matrix, homogeneous transformation matrix and D-H notation are also utilized.

The stability of the robot is analyzed by using ZMP criteria. To calculate ZMP, the individual link accelerations are needed. An iteration method is proposed to apply for this model to calculate link linear accelerations and to stabilize the robot when walking, a ZMP based method is proposed.

16

Chapter 3

Swing Leg Kinematics of Bipedal Robot

3.1 Preliminaries

To modeling of swing leg kinematics it is needed to study the basic robotics theories[18]. These theories can be utilized to derive joint angle equations. Application of the basic robotic theory to solve real world problem is one of the goals of this research. In this research, both legs are considered as planer manipulators. Hence, studying of manipulator kinematics is much important for derivation of kinematics model.

3.1.1 Manipulator kinematics

Kinematics is the science of motion which treats motion without regard to the forces which cause it. Within the science of kinematics one studies the position, velocity, acceleration, and all higher order derivatives of the position variables (with respect to time or any other variable(s)). Hence, the study of the kinematics of manipulators refers to all the geometrical and time based properties of the motion. The relationship between these motions and the forces and torques which cause them the problem of dynamics.

In order to deal with the complex geometry of a manipulator it will affix frames to the various parts of the mechanism and then describe the relationship between these frames. The study of manipulator kinematics involves, among other things, how the locations of these frames change as the mechanism articulates. The method mentioned in this sub topic is to compute the position and orientation of the manipulator's end-effector relative to the base of the manipulator as a function of the joint variables.

3.1.2 Link Description

A manipulator may be thought of as a set of bodies connected in a chain by joints. These bodies are called links. Each joint usually exhibits one degree of freedom. Most manipulators have joints which are like hinges, called revolute joints, or have sliding joints called prismatic joints. In the rare case that a mechanism is built with a joint having n degrees of freedom, it can be modeled as n joints of one degree freedom connected with $n-1$ links of zero length. Therefore, without loss of generality, it will consider only manipulators which have joints with a single degree of freedom.

The links are numbered starting from the immobile base of the arm, which might be called link 0. The first moving body is link 1, and so on, out to the free end of the arm , which is link n. In order to position end-effector generally in 3-space, a minimum of 6

joints are required. Typical manipulators have 5 or 6 joints. Some robots may actually not be as simple as a single kinematic chain-they may have parallelogram linkages or other closed kinematic structures.

A single link of a typical robot has many attributes which a mechanical designer had to consider during its design. These include the type of material used, the strength and stiffness of the link, the location and type of the joint bearing, the external shape, the weight and inertia etc. However, for the purposes of obtaining the kinematics equations of the mechanism, *a link is considered only as a rigid body which defines the relationship between two neighboring joint axes of a manipulator.* Joint axes are defined by lines in space. Joint axis i is defined by a line in space, or a vector direction, about which i rotates relative to link $i-1$. It turns out that for kinematic purposes, a link can be specified with two numbers which define the relative location of the two axes in space.

For any two axes in 3-space there exists a well-defined measure of distance between them. This distance is measured along a line which us mutually perpendicular to both axes. This mutual perpendicular always exists and is unique except when both axes are parallel, in which case there are many mutual perpendicular of equal length. Figure (3.1) shows link $i-1$ and the mutually perpendicular line along which the **link length**, a_{i-1} is measured. The second parameter needed to define the relative location of the two axes is called the **link twist**. If we imagine a plane whose normal is the mutually perpendicular line just constructed, it can be projected that both axes $i-1$ and i onto this plane and measure the angle between them. This angle is measured from axis $i-1$ to axis i in the right hand sense about a_{i-1}. We will use this definition of the twist of link $i-1$, α_{i-1}. In Figure(3.1) α_{i-1} is indicated as the angle between axis $i-1$ and axis i.
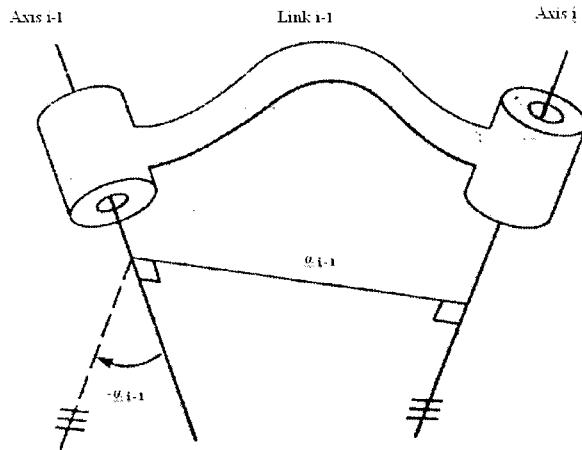
Figure 3.1: Relationship of link length and link twist

18

3.1.3 Link parameters

Any robot can be described kinematically by giving the values of four quantities for each link. Two describe the link itself, and two describe the link's connection to a neighboring link. In the usual case of a revolute joint, θ_i is called the joint variable, and the other three quantities would be fixed link parameters as shown in Figure (3.2). For prismatic joints, d_i is the joint variable and the other three quantities are fixed link parameters. The definition of mechanisms by means of these quantities is a convention usually called the Denavit-Hartenberg notation.
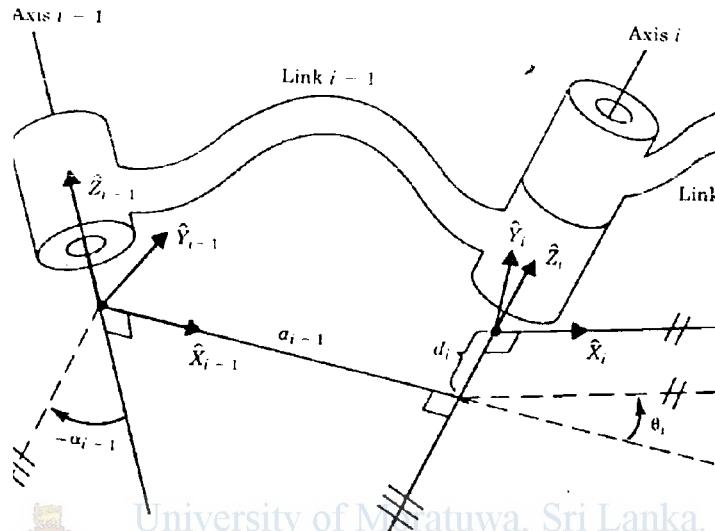
Figure 3.2: Parameters used to describe the connecting between neighboring links

That $\theta_n = 0.0$ and the origin of frame {N} is chosen at the intersection of $\hat{X}_{N-1}$ and joint axis n when $d_n = 0.0$

If the link frames have been attached to the links according to our convention, the following definitions of the link parameters are valid.

a_i = the distance from $\hat{Z}_i$ to $\hat{Z}_{i+1}$ measured along $\hat{X}_i$,

α_i = the angle between $\hat{Z}_i$ and Z_{i+1} measured about $\hat{X}_i$,

d_i = the distance from $\hat{X}_{i-1}$ to $\hat{X}$ measured along $\hat{Z}_i$ and

θ_i = the angle between $\hat{X}_{i-1}$ and $\hat{X}_i$ measured about $\hat{Z}_i$

We usually choose $a_i \rangle 0$ since it corresponds to a distance, however, α_i, d_i and θ_i are signed quantities.

19

The convention outlined above does not result in a unique attachment of frames to links. First of all, when we first align the $\hat{Z}_i$ axis with joint axis i, there are two choices of direction in which to point $\hat{Z}_i$. Furthermore, in the case of intersecting joint axes (i.e. $a_i = 0$), there are two choices for the direction of $\hat{X}_i$, corresponding to the choice of signs for the normal to the plane containing $\hat{Z}_i$ and $\hat{Z}_{i+1}$. Also, when prismatic joints are present there is quite a bit of freedom in frame assignment.

3.1.4   Derivation of link transformations

Determination of the transform which defines frame $\{i\}$ relative to the frame $\{i-1\}$. In general, this transformation will a function of the four link parameters. For any given robot, this transformation will be a function of only one variable, the other three parameters being fixed by mechanical design. By defining a frame for each link we have broken the kinematics problem into n sub problems. In order to solve each of these sub problems, namely $^{i-1}_iT$, we will further break the problem into four sub-subproblems. Each of these four transformations will be a function of one link parameter only, and will be simple enough that we can write down its form by inspection. We begin by defining three intermediated frames for each link, namely: $\{P\}$, $\{Q\}$, and $\{R\}$.
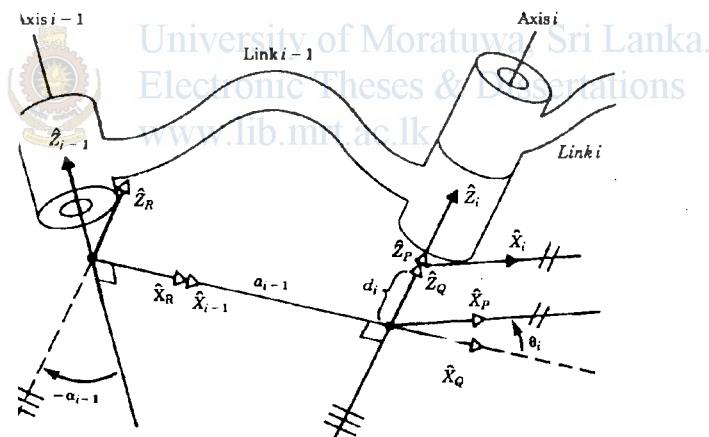
Figure 3.3: Attachment of frame $\{i\}$ rigidly to the link i

Figure (3.3) shows the same pair of joints as before with frames $\{P\}, \{Q\}$ and $\{R\}$ defined. Note that only the $\hat{X}$ and $\hat{Z}$ axes are shown for each frame to make the drawing clearer. Frame $\{R\}$ differs from frame $\{i-1\}$ only by a rotation of α_{i-1}. Frame $\{Q\}$ differs from $\{R\}$ by a translation a_{i-1}. Frame $\{P\}$ differs from $\{Q\}$ by a rotation θ_i, and frame $\{i\}$ differs from $\{P\}$ by a translation d_i. If we wish to write the transformation which transforms vectors defined in $\{i\}$ to their description in $\{i-1\}$ we may write

$$P = {}^{i-1}_R T \; {}^R_Q T \; {}^Q_P T \; {}^P_i T \; {}^i p \tag{3.1}$$

or

$${}^i P = {}^{i-1}_i T \; {}^i P \tag{3.2}$$

where

$$T = {}^{i-1}_R T \; {}^R_Q T \; {}^Q_P T \; {}^P_i T \tag{3.3}$$

Considering each of these transformations the equation written as:

$$T = Rot(\hat{X}_i, \alpha_{i-1}) \; Trans(\hat{X}_i, \alpha_{i-1}) \; Rot(\hat{Z}_i, \theta_i) \; Trnas(\hat{Z}_i, d_i) \tag{3.4}$$

or

$$T = Screw(\hat{X}_i, a_{i-1}, \alpha_{i-1}) Screw(\hat{Z}_i, d_i, \theta_i) \tag{3.5}$$

Where Screw ($\hat{Q}, r, \Phi$) stands for a translation along an axis $\hat{Q}$ by a distance r, and a rotation about the same axis by an angle Φ. Multiplying out (3.4) we obtain the general form of ${}^{i-1}_i T$.

$$T_i = \begin{bmatrix} C\theta_i & -S\theta_i & 0 & a_{i-1} \\ S\theta_i C\alpha_{i-1} & C\theta_i C\alpha_{i-1} & -S\alpha_{i-1} & -S\alpha_{i-1}d_i \\ S\theta_i S\alpha_{i-1} & C\theta_i S\alpha_{i-1} & C\alpha_{i-1} & C\alpha_{i-1}d_i \\ 0 & 0 & 0 & 1 \end{bmatrix} \tag{3.6}$$

3.1.5 Concatenating link transformations

Once the link frames have been defined and the corresponding link parameters found, developing the kinematic equations is straight forward. Using the values of the link parameters the individual link transformation matrices can be computed. Then, the link transformations can be multiplied together to find the single transformation that relates frame $\{N\}$ to frame $\{0\}$:

$${}^0_N T = {}^0_1 T \; {}^1_2 T \; {}^2_3 T ... {}^{N-1}_N T \tag{3.7}$$

This transformation, ${}^0_N T$ will be a function of all n joint variables. If the robot's joint position sensors are queried, the Cartesian position and orientation of the last link may be computed by ${}^0_N T$.

3.2 Derivation of joint angle equations for swing leg

To derive the joint angle equations, the direct kinematics and inverse kinematics theories are used.
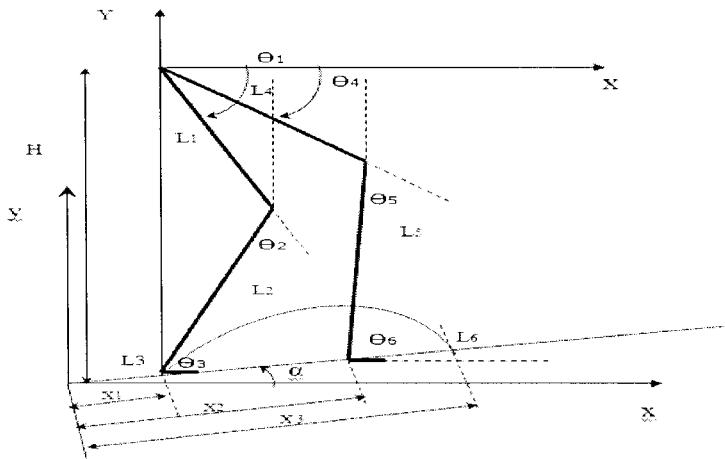
Figure 3.4: Robot lower body and nomenclature

By utilizing the link description theories and by inspecting the above diagram the D-H table of swing leg can be obtained as:

	α_{i-1}	a_{i-1}	d_{i-1}	θ_{i-1}
1	0	0	0	$-\theta_1$
2	0	L_1	0	$-\theta_2$
3	0	L_2	0	$-\theta_3$

Table 3.1: D-H parameters of swing leg

For a planer serial manipulator the link transformation matrix is given by the equation (3.6) as,

$$
{}^{i-1}_iT = \begin{bmatrix} C\theta_i & -S\theta_i & 0 & a_{i-1} \\ S\theta_iC\alpha_{i-1} & C\theta_iC\alpha_{i-1} & -S\alpha_{i-1} & -S\alpha_{i-1}d_i \\ S\theta_iS\alpha_{i-1} & C\theta_iS\alpha_{i-1} & C\alpha_{i-1} & C\alpha_{i-1}d_i \\ 0 & 0 & 0 & 1 \end{bmatrix}
$$

In this swing leg, number of links are 3. Therefore the individual link transformation matrix can be obtained by substituting i=1,2,3 for general equations as:

22

$i = 1$

$$_1^0T = \begin{bmatrix} C\theta_1 & -S\theta_1 & 0 & 0 \\ S\theta_1 & C\theta_1 & 0 & 0 \\ 0 & 0 & 1 & 0 \\ 0 & 0 & 0 & 1 \end{bmatrix}$$

$i = 2$

$$_2^1T = \begin{bmatrix} C\theta_2 & -S\theta_2 & 0 & L_1 \\ S\theta_2 & C\theta_2 & 0 & 0 \\ 0 & 0 & 1 & 0 \\ 0 & 0 & 0 & 1 \end{bmatrix}$$

and

$$_3^2T = \begin{bmatrix} C\theta_3 & -S\theta_3 & 0 & L_2 \\ S\theta_3 & C\theta_3 & 0 & 0 \\ 0 & 0 & 1 & 0 \\ 0 & 0 & 0 & 1 \end{bmatrix}$$

Then the matrix $_3^0T$ can be derived by using the relationship in equation (3.7) as

$$_3^0T = {}_1^0T \times {}_2^1T \times {}_3^2T$$

Simplifying to,

$$_3^0T = \begin{bmatrix} C\theta_{123} & -S\theta_{123} & 0 & L_2C\theta_{12} + L_1C\theta_1 \\ -S\theta_{123} & C\theta_{123} & 0 & -[L_2S\theta_{12} + L_1S\theta_1] \\ 0 & 0 & 1 & 0 \\ 0 & 0 & 0 & 1 \end{bmatrix}$$

$$C\theta = \cos\theta, \; C\theta_{123} = \cos(\theta_1 + \theta_2 + \theta_3)$$
$$S\theta = \sin\theta, \; S\theta_{123} = \sin(\theta_1 + \theta_2 + \theta_3)$$

This is the homogeneous transformation matrix for the swing leg.

23

3.2.1 Derivation of equation for joint angle θ_2

To perform inverse kinematics operation it is needed to suggest end effecter matrix as below

$$\begin{bmatrix} \cos\phi & -\sin\phi & 0 & X \\ -\sin\phi & \cos\phi & 0 & -Y \\ 0 & 0 & 1 & 0 \\ 0 & 0 & 0 & 1 \end{bmatrix} \quad \begin{aligned} X &= X - x_1 Cos\alpha \\ Y &= -[H + x_1 Sin\alpha - y] \end{aligned}$$

This model can be utilized if known parameters are pose and orientation and unknowns are join parameters.

Pose and Orientation $\longrightarrow$ | Inverse kinematics Model | $\longrightarrow$ Joint Parameters
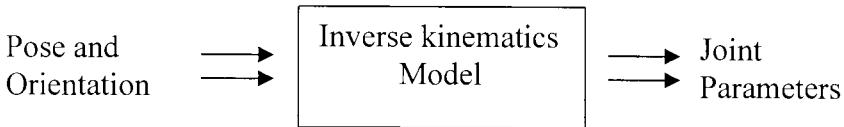
In swing leg kinematics model we know the pose and orientation of the foot (end effecter) utilizing trajectory generation, unknowns are joint angles. Hence inverse kinematics model is suitable to solve this problem. By using inverse kinematics, that is equating homogeneous transformation matrix and end effecter matrix the following two equations can be obtained.

By equating,

- Element (4,1) of homogeneous transformation matrix and (4,1) of end effecter matrix
- Element (4,2) of homogeneous transformation matrix and (4,2) of end effecter matrix

$$X = L_2 C_{12} + L_1 C_1$$

$$Y = L_2 S_{12} + L_1 S_1$$

Square X and Y then adding

$$\cos\theta_2 = \left[\frac{X^2 + Y^2 - L_1^2 - L_1^2}{2L_1 L_2} \right] = C_2$$

$$Then \ S_2 = \stackrel{+}{-}\sqrt{1 - \cos^2\theta_2}$$

$$\theta_2 = A\tan 2 \left[S_2, C_2 \right] \tag{3.8}$$

The function A tan 2[S_2 ,C_2] represent $\tan^{-1}(S_2/C_2)$. But, uses the sign of both S_2 and C_2 to determine the quadrant in which the resulting angle lies.

3.2.2 Derivation of equation for joint angle θ_1

After derived θ_2, we have to derived an equation for θ_1.

$$X = L_1 C_1 + L_2 C_{12} \tag{3.9}$$
$$Y = L_1 S_1 + L_2 S_{12} \tag{3.10}$$

Re-writing the X and Y, by introducing K_1, K_2.

$$X = K_1 C_1 - K_2 S_1 \tag{3.11}$$
$$Y = K_1 S_1 + K_2 C_1 \tag{3.12}$$

Where

$$K_1 = L_1 + L_2 C_2$$
$$K_2 = L_2 S_2$$

Performing change of variables

If, $r = \sqrt{(K_1^2 + K_2^2)}$

And $\gamma = A\tan 2(K_2, K_1)$

Then
$$K_1 = r\cos\gamma$$
$$K_2 = r\sin\gamma$$

The equation (3.11) and (3.12) can be rewrite as,

$$\tfrac{X}{r} = \cos\gamma\cos\theta_1 - \sin\gamma\sin\theta_1$$
$$\tfrac{Y}{r} = \cos\gamma\sin\theta_1 + \sin\gamma\cos\theta_1$$
$$\cos(\gamma + \theta_1) = \tfrac{X}{r}$$
$$\sin(\gamma + \theta_1) = \tfrac{Y}{r}$$
$$\therefore \quad \gamma + \theta_1 = A\tan 2[\tfrac{Y}{r}, \tfrac{X}{r}]$$

then,
$$\theta_1 = A\tan 2[Y, X] - A\tan 2[K_2, K_1] \tag{3.13}$$

3.2.3   Derivation of equation for joint angle θ_3

After derivation of θ_1 and θ_2 the angle θ_3 can be obtained using the concept "In a serial manipulator the last joint angle is equal to total of previous joint angles"
Therefore,
$$\theta_3 = \theta_1 + \theta_2 + \alpha \tag{3.14}$$
Where α is the angle of slope.

Chapter 4

Gait Development

Before a bipedal robot can walk, a gait or walking pattern must be developed for the robot to follow. There are many different ways [19] of doing this, however the aim of gait development is to produce a gait which is dynamically stable. If the gait is dynamically stable, when the robot walks according to the gait in the absence of external disturbances, it will achieve dynamic walking. However, if the gait is not dynamically stable then the robot will fall over, since the system will be unstable.

Walking is a repetitive motion, which consists of two main phases which alternate on each leg:

1. Double support phase
   This phase exists when both feet are in solid contact with the ground plane. In this phase the robot is stable with a relatively large support base. The system enters this state when the front foot contacts the ground, and leaves this state when the rear foot breaks contact with the ground.

2. Single support phase or swing phase
   This phase exists where only one foot is in solid contact with the ground plane. During this phase the centre of mass (COM) of the robot rotates about this contact point in the manner of an inverse pendulum, while the other leg known as the swing leg translates in preparation to come in contact with the ground for the next double support phase. The systems enters this state when the swing leg foot breaks contact with the ground and leaves this state when the swing leg foot contacts the ground.

This cycle can be seen in Figure (4.1). As can be seen from the state diagram, the walking pattern alternates the single support phases between each leg, interspersed with a double support phase between each alternation.
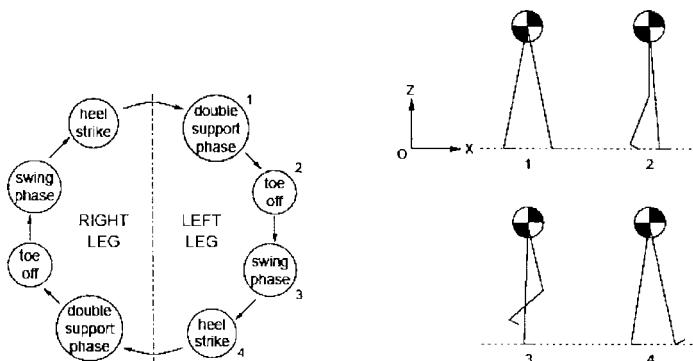

Figure 4.1: Illustration of the gait cycle and dynamic biped walking

Some different approaches to gait development are discussed below.

4.1   Intuitive approach

The intuitive approach to gait development is not directly based upon dynamic principles, rather it is more a method of building one step of the gait at a time. This is achieved by experimental modification of the gait by examining the performance of the gait on the robot. This approach, has no previously known data to compare the performance of the robot against, and therefore we cannot generate a performance measure for the gait. Without such a quantitative measure we can only observe the robot while it is enacting the gait to determine the stability of the gait. For this reason the approach is called intuitive.

This method was chosen first to develop a gait due to its simple nature. The analytical approaches are complex and often have no solution or no unique solution. An intuitive approach allows the consideration of more subjective measures such as developing the gait through examination of the human gait, which is highly efficient.

In this way, through many trials and examinations of the behaviour of the robot, an intuitive understanding is built up which allows a reasonable dynamically stable gait to be developed. Using this method, joint angles were determined over time, and allowed the robot to take three steps before falling over without feedback and control. This shows that although the intuitive approach is not as objective and theoretically grounded in the dynamics of the robot system, it can be successful in allowing a dynamically stable gait to be rapidly developed. Of more importance is the experience and understanding of the system which was gained through this method.

4.2   Periodic function approach

One major drawback to the intuitive approach is that the gait which is developed is not easily scalable. For example, parameters which we might like to alter such as step length, step height or step period cannot easily be altered offline, and are even more difficult to alter while the robot is in motion.

To understand why we would want such parameters, we need to consider the entire walking cycle. The walking cycle begins with the robot stationary, and accelerates to the desired velocity. The cycle ends with the robot decelerating and eventually coming to rest. In order to vary the velocity, we require a method of scaling the gait under different situations. In this manner, we can develop a single set of joint angle relationships over time that completely specify the walking gait and allow the variation of the desired parameters.

Since walking is a repetitive motion which repeats over time, we use periodic functions as a basis for developing the gait. In this way, we can specify the period of the step. Further, in order to specify parameters for changing the step length and step height, we specify the trajectory of the foot over time. This allows us to solve for the required angles of the leg link joint angles.

4.3 Foot trajectory

As mentioned above, specifying the foot trajectory over time allows the parameters of step length and step height to be introduced to the gait. Using inverse kinematics, we can then solve for the joint angles of the leg links over time, thereby specifying the gait.

When considering the foot trajectory, we consider the period as one step. In this way we only need to consider the swing leg foot trajectory since the support leg foot is in contact with the floor, and therefore stationary. We can specify any trajectory as below;

(i)   use of a p-degree polynomial as interpolation function
(ii) cubic polynomial trajectories
(iii) Linear function with parabolic blends

In this research, cubic polynomial trajectory is selected to describe the path of the ankle of swing leg as,

$$y = a_0 + a_1 x + a_2 x^2 + a_3 x^3$$

To describe the foot trajectory the constants a_0, a_1, a_2, a_3 need to be found. To find out the constants following known x and y values can be used. By substituting these known values to the cubic polynomial equation a relationship between x and y is obtained.

At $x = x_1 \cos\alpha$, $\quad y = x_1 \sin\alpha$

At $x = (x_1 \cos\alpha + x_2 \cos\alpha)/2$, $\quad y = x_2 \sin\alpha + f/2$

At $x = (x_2 \cos\alpha + x_3 \cos\alpha)/2$ $\quad y = x_3 \sin\alpha + f/2$

At $x = x_3 \cos\alpha$, $\quad y = x_3 \sin\alpha$

To find out the y values relative to the different x values the above relation is used.

Chapter 5

Stance Leg Kinematics

5.1   Stance leg modeling

In robotic modeling, the implementation of stance foot kinematics model is important since,

    (i)   the cyclic gait requirements depend on this modeling
    (ii)   the movement of the hip in forward direction is based on the stance foot kinematics modeling

Therefore, the stance foot is need to be orientated its joints according to move the hip in forward direction while performing the swinging operation simultaneously. The time period must be similar for both cases.

5.2 Mathematical modeling
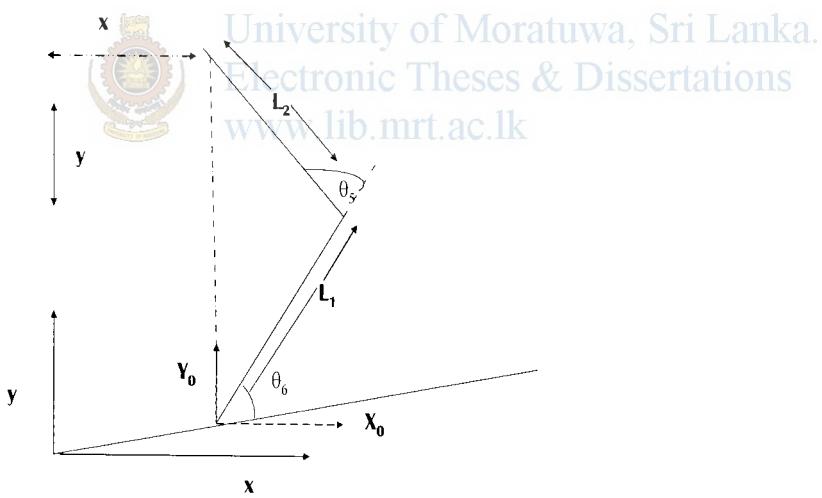
Figure 5.1: Stance leg and nomenclature

5.2.1   DH parameters for stance leg

In this modeling, the stance leg is also assumed to be a serial link planer manipulator in which its base is ankle and end effector being hip. In this case, the number of link is equal to two since the stance foot is stationary.

29

i	α_{i-1}	a_{i-1}	d_i	θ_1
1	0	0	0	θ_6
2	0	L_1	0	θ_5
3	0	L_2	0	0

Table 5.1: DH parameters of stance leg

In this case $\theta_3 = 0$ as there is no 3$^{\text{rd}}$ link.

5.2.2 Link transformation, homogeneous transformation and end effector matrices for stance leg

To obtain homogeneous transformation matrix for the stance leg it is needed to derive individual link transformation matrix, using the equation (3.6), the general form of link transformation matrix is,

$$
{}^{i-1}_{i}T = \begin{bmatrix}
C\theta_i & -S\theta_i & 0 & a_{i-1} \\
S\theta_i C\alpha_{i-1} & C\theta_i C\alpha_{i-1} & -S\alpha_{i-1} & -S\alpha_{i-1}d_i \\
S\theta_i S\alpha_{i-1} & C\theta_i S\alpha_{i-1} & C\alpha_{i-1} & C\alpha_{i-1}d_i \\
0 & 0 & 0 & 1
\end{bmatrix}
$$

and the D-H table for stance leg, ${}^{0}_{1}T$, ${}^{1}_{2}T$, ${}^{2}_{3}T$ can be calculated as

$i = 1$

$$
{}^{0}_{1}T = \begin{bmatrix}
c\theta_6 & -s\theta_6 & 0 & 0 \\
s\theta_6 & c\theta_6 & 0 & 0 \\
0 & 0 & 1 & 0 \\
0 & 0 & 0 & 1
\end{bmatrix}
$$

$i = 2$

$$
{}^{1}_{2}T = \begin{bmatrix}
c\theta_5 & -s\theta_5 & 0 & L_1 \\
s\theta_5 & c\theta_5 & 0 & 0 \\
0 & 0 & 1 & 0 \\
0 & 0 & 0 & 1
\end{bmatrix}
$$

30

$$\begin{bmatrix} 1 & 0 & 0 & L_2 \\ 0 & 0 & 0 & 0 \\ 0 & 0 & 1 & 0 \\ 0 & 0 & 0 & 1 \end{bmatrix}$$

The homogeneous transformation matrix ${}^0_3T$ can be obtained as:

$${}^0_3T = {}^0_1T \times {}^1_2T \times {}^2_3T$$

as

$${}^0_3T = \begin{bmatrix} \cos(\theta_6 + \theta_5) & -\sin(\theta_6 + \theta_5) & 0 & L_1 \cos\theta_6 + L_2 \cos(\theta_6 + \theta_5) \\ \sin(\theta_6 + \theta_5) & \cos(\theta_6 + \theta_5) & 0 & L_1 \sin\theta_6 + L_2 \sin(\theta_6 + \theta_5) \\ 0 & 0 & 1 & 0 \\ 0 & 0 & 0 & 1 \end{bmatrix} \tag{5.1}$$

To apply inverse kinematics, it is needed to define the end effector matrix for this stance leg. That is the matrix that describes position and orientation of the hip reference to the ankle. By inspecting the pattern of the homogeneous transformation matrix it can be proposed that,

$$\begin{bmatrix} \cos\phi & -\sin\phi & 0 & -X_0 \\ \sin\phi & \cos\phi & 0 & Y_0 \\ 0 & 0 & 1 & 0 \\ 0 & 0 & 0 & 1 \end{bmatrix} \tag{5.2}$$

as the end effector matrix.

Where ϕ represents the orientation of the hip reference to the $-X_0$ axis and (x_0, y_0) is the coordinates of hip.

5.2.3 Derivation of joint angle equations

This derivation is based on the inverse kinematics theory. In inverse kinematics, the homogeneous transformation matrix can be equal to end effector matrix.

By equating element (1,4) of homogeneous transformation matrix (5.1) to element (1,4) of end effector matrix(5.2) the following expression can be obtained.

$$X_0 = -\left[L_1 \cos\theta_6 + L_2 \cos(\theta_6 + \theta_5) \right] \tag{5.3}$$

By equating element (2,4) of homogeneous transformation matrix(5.1) to element (2,4) of end effector matrix(5.2) the expression for Y_0 is as below;

31

$$Y_0 = L_1 \sin\theta_6 + L_2 \sin(\theta_6 + \theta_5) \tag{5.4}$$

By squaring (5.3) and (5.4), then adding

$$X_0^2 + Y_0^2 = [L_1 \cos\theta_6 + L_2 \cos(\theta_5 + \theta_6)]^2 + [L_1 \sin\theta_6 + L_2 \sin(\theta_6 + \theta_5)]^2$$

$$\cos\theta_5 = \frac{X_0^2 + Y_0^2 + L_1^2 + L_2^2}{2L_1 L_2}$$

Therefore,

$$\sin\theta_5 = \sqrt{1 - \cos\theta_5} \tag{5.5}$$

$$\theta = A \tan 2 [S_5, C_5]$$

5.3   Modification of swing leg kinematics

When derivation of kinematic model for swing leg, it is assumed that the "swing leg is equal to 3 link planner manipulator and it's stationary base is hip and end effector is ankle". In stance leg model derivations, it is assumed that the "stance leg is a 2-link planner manipulator whose stationary base is ankle and moving end effector is hip". These two cases create a contradiction i.e. in first case hip is considered as fixed but, in second case it is moving. To avoid this contradiction, the swing leg kinematics model is need to be modified by adding another co-ordinate frame to hip in first case as illustrated by the Figure 5.2
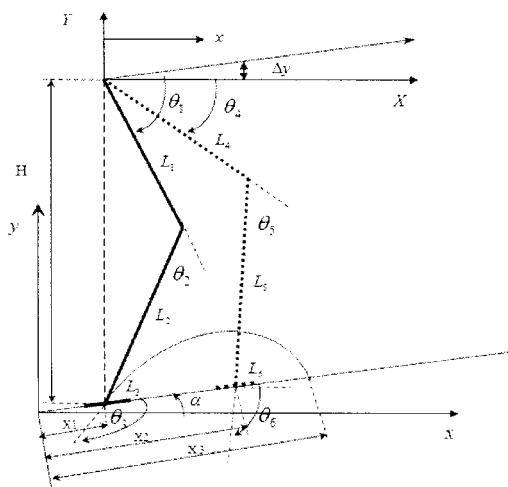
Figure 5.2: Robot lower body with moving hip

In this modification X and Y coordinates are modified as,

$$X = (x - x_1 \cos\alpha) - x' \tag{5.6}$$

$$Y = (H + x_1 \sin\alpha - y) + \Delta y \tag{5.7}$$

Where, x' is the horizontal hip movement from initial point and Δy is the vertical hip movement from initial point.

5.3.1 Trajectory planning of hip

In previous case, it is noted that the hip is also moving simultaneously with swing leg operation. Therefore, it is needed to predefine the hip trajectory.

To plan hip trajectory, the rimless wheel simulation can be adopted.

5.3.2 Rimless wheel simulation

In rimless wheel simulation [20] it is considered a wheel with spokes and rim. When rolling the wheel, it can be seen that the trajectory of the centre of the wheel is straight line. In the case of rimless wheel simulation, the trajectory of the centre is not a straight line. If number of spokes increases, this trajectory closes to a straight line as illustrated in Figure 5.3

Trajectory of the center of the wheel
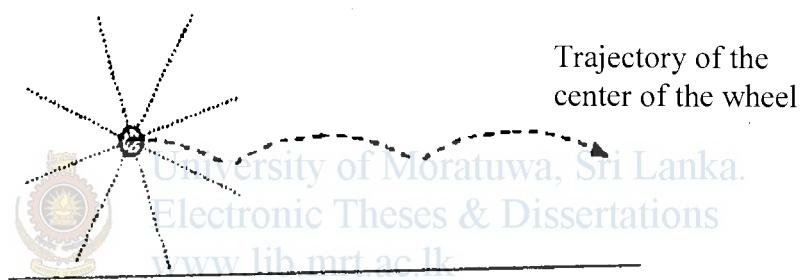
Figure 5.3: The simulation of rimless wheel

By applying this concept for hip trajectory planning, it can be assumed that the hip trajectory is a straight line. In the case of ramp walking, the hip trajectory is a straight line parallel to the sloping surface.
Then the equation for θ_6 can be derived as follows,
By rimless wheel simulation result, it can be assumed that,
$$\Delta H = (\tan \alpha).x \tag{5.8}$$

Performing change of variables and introducing K1 and K2 θ_6 can be found as,

$$\theta_6 = A \tan 2(Y_0, X_0) - A \tan 2(K_1, K_2) \tag{5.9}$$

Where, X_0, Y_0 as above (5.6) and (5.7)

$K_1 = L_1 + L_2 \cos \theta_5$

$K_2 = L_2 \sin \theta_5$

In bipedal walking cyclic gait concept is important since it repeats the robot position of each walking cycle. Due to this repetition the equations derived for one walking cycle can be used for the other walking cycles also. The basic requirement for cyclic gait is as follows;

[Initial pose of swing leg] = [Final pose of stance leg]

$[\theta_2]_{initial} = [\theta_5]_{final}$

$[\theta_3]_{initial} = [\theta_6]_{final}$

If these requirements are satisfied, the stance leg becomes swing leg in the next gait cycle and vice versa.

5.3.3 Calculations of hip movement

When swing leg moves one step length it is needed to find the distance of hip movement to maintain cyclic gait requirements. In this research, used a graphical method to find hip movement distance. The steps of this graphical method are as follows.

1. Find initial pose of the stance leg, using the equations derived for θ_5 and θ_6. To find initial position it needs X_0 and Y_0 terms as

$$X_0 = x - [x_2 - x_1]\cos\alpha$$
$$Y_0 = H - [x_2 - x_1]\sin\alpha + \Delta H$$

Substituting initial condition, $x = 0$ and $\Delta H = 0$

θ_5 and θ_6 can be calculated utilizing the equations (5.5) and (5.9)

2. Find initial pose of swing leg using the equations (3.8) and (3.13) derived for θ_3 and θ_2 and equations for x and y with following initial conditions.
$$x = x_1 \cos\alpha, \; y = x_1 \sin\alpha$$
$$x = 0$$
$$\Delta y = 0$$

3. Equate final pose of stance leg to initial pose of swing leg and obtain θ_5 and θ_6 final values.

4. Drawing the two positions of stance foot and measure the hip movement distance.

By using this graphical method it can be verified that the hip movement distance is equivalent to half of the step length.

Chapter 6

Dynamic Stability Analysis for Lower Body

6.1 Methods for stability analysis of biped robots

The dynamic stability can be analyzed in bipedal robot utilizing two methods as:

(1)   COM-centre of mass
(2)   ZMP-Zero Moment Position

According to the literature survey of bipedal walking, the common method that used to analyze dynamic stability is ZMP method. Therefore, as previous, the ZMP is used to analyze the dynamic stability in this research.

6.1.1   Zero Moment Position

The ZMP is the most commonly used concept for bipedal stability analysis which was invented by Prof. Miomir at Serbia in 1972 [21]. Let us consider the single support phase as shown in Figure (6.1), i.e. the case when only one foot is in contact with the ground (stance leg) while the other is in the swing phase, relatively passing from the back to the front position. To maintain the mechanism's dynamic equilibrium, the ground reaction force R should act as the appropriates point on the foot sole to balance all the forces acting on the mechanism during motion (inertial, gravitational, Coriolis and centrifugal forces and the corresponding moments), as shown in Figure (6.1).
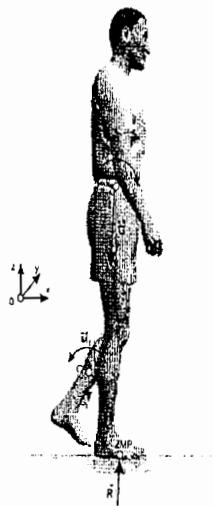
Figure 6.1: Single support phase

35

If we place the coordinate system at the point where R is acting (let us assume for a moment that this point is under the foot), it is clear from the equilibrium conditions that the moments acting about the horizontal axes x and y will always be equal to zero, ie. $M_x = 0$ and $M_y = 0$. The only moment component that may exist is M_z. It is a very realistic assumption that the M_z is balanced by friction forces. since the both moments relative to the gait continuation(M_x and M_y) are equal zero, a natural choice to name the ground reaction force acting at this point will be zero-moment point. Any change in the locomotion dynamics will change the vector of the ground reaction force, causing simultaneous changes in its direction, intensity, and acting point (ZMP position).

The following basic ZMP definition reflects the above consideration.

Definition1 (The notion of the ZMP): The pressure under supporting foot can be replaced by the appropriate reaction force acting at a certain point of the mechanism's foot. Since the sum of all moments of active forces with respect to this point is equal to zero, it is termed the zero-moment point (ZMP)

In order to define ZMP in a mathematical form let us consider the dynamic model of the biped locomotion system. The robot dynamics will be modeled using the multi-body system model consisting of N chains involving the body parts. Each chain consist of n rigid links $i = 1,...,N$) interconnected with single DOF joints. During locomotion the following active motion forces act on the body links: $\vec{G}_i$-gravitation force of the i-th link acting at the mass centre C_i, $\vec{F}_i$-inertial force of the i-th link acting at the mass centre C_i, $\vec{M}_i$-moment of the inertial fore of the i-th link for C_i, $\vec{R}$ resultant ground reaction force.

All active motion forces (gravitational and inertial forces and moments) can be replaces by the main resultant gravitation and inertial force and, in general case, the resultant inertial moment reduced at the body centre of mass (COM). The ground reaction force and moment can be decomposed into the vertical and horizontal components with respect to the reference frame in the following way

$$R = \vec{R}_v + \vec{R}_f S$$

$$M = \vec{M}_h + \vec{M}_f$$

Where the indices h and v denote the horizontal and vertical components respectively, while f indicates the friction reaction force and moment components. The following equations describe the dynamic equilibrium during the motion in the reference coordinate system if we select the ZMP as the reduction point of interest

36

$$\vec{R}_v + \vec{R}_f + \sum_{j=1}^{N} \sum_{i=1}^{n_j} (\vec{F}_i + \vec{G}_i) = 0$$

(6.1)

$$\overrightarrow{OZMP} \times \vec{R} + \sum_{j=1}^{N} \sum_{i=1}^{n_j} \overrightarrow{OC_i} \times (\vec{F}_i + \vec{G}_i) + \sum_{j=1}^{N} \sum_{i=1}^{n_j} \vec{M}_i + \vec{M}_{hZMP} + \vec{M}_{fZMP} = 0$$

Where O denotes the origin of the reference frame (Figure 6.1). Then, based on the ZMP definition we have

$$\vec{M}_{hZMP} = 0$$

Substituting the relation

$$\overrightarrow{OC_i} = \overrightarrow{OZMP} + \overrightarrow{ZMPC_i}$$

(6.2)

Into the second equation of (7.1) and taking into account the first equation of (7.1) gives

$$\sum \sum_{i=1}^{n_j} \overrightarrow{ZMPC_i} \times (\vec{F}_i + \vec{G}_i) + \sum_{j=1}^{N} \sum_{i=1}^{n_j} \vec{M}_{fZMP} = 0$$

(6.3)

Considering only the dynamic moment equilibrium in the horizontal ground plane (i.e. the moments that are not compensated by friction) we can write

$$\left[\sum \sum_{i=1}^{n_j} \overrightarrow{ZMPC_i} \times (\vec{F}_i + \vec{G}_i) + \sum_{j=1}^{N} \sum_{i=1}^{n_j} \vec{M}_i \right]_h = 0$$

(6.4)

Substituting (6.2) in (6.4) we get

$$\left[\overrightarrow{OZMP} \times \sum_{j=1}^{N} \sum_{i=1}^{n_j} (\vec{F}_i + \vec{G}_i) \right]_h = (\vec{R} \times \overrightarrow{OZMP})_h = \left(\sum_{j=1}^{N} \sum_{i=1}^{n_j} \overrightarrow{OC_i} \times (\vec{F}_i + \vec{G}_i) + \sum_{j=1}^{N} \sum_{i=1}^{n_j} \vec{M}_i \right)$$

(6.5)

Equations (6.4) and (6.5) represent the mathematical interpretation of ZMP and provide the formalism for computing the ZMP coordinates in the ground plane. Finally an equation for ZMP can be obtained as

$$X_{ZMP} = \sum_{i=1}^{i=4} \frac{(I_i \dot{\omega}_i + m_i x_i (\ddot{y}_i - g) - m_i \ddot{x}_i y_i)}{\sum_{i=1}^{i=4} m_2 (\ddot{y}_i - g)}$$

Where

X_{ZMP} -Distance to the ZMP in x direction from (x,y) coordinate frame.

I - *Moment of inertia of each link*

$\dot{\omega}$ *Angular accelaration of each link*

m *Weight of each link*

$\ddot{x}$ *Linear accelaration of linki in X direction*

$\ddot{y}$ *Linear accelaration of linki in Y direction*

6.2   ZMP calculation for lower body

To check the dynamic stability of derived lower body model it is essential to calculate ZMP. The commonly used equation for ZMP as

$$X_{ZMP} = \sum_{i=1}^{i=4} \frac{(I_i\dot{\omega}_i + m_i x_i(\ddot{y}_i - g) - m_i \ddot{x}_i y_i)}{\sum_{i=1}^{i=4} m_2(\ddot{y}_i - g)}$$

Utilizing the above equation, it is very complex to calculate the ZMP for the lower body of the robot. Following is the remedies to avoid complexity.

1. The foot of stance leg is not moving during that gait cycle, hence this foot link can be omitted for ZMP calculation.
2. It can be shown that the effect on ZMP from foot link of swing leg is negligible. Therefore, the total number of links can be reduced from 6 to 4.
3. The each term of the equation can be calculated separately and finally substitute to the original equations.

The separate terms are as below;

1. Inertia terms (I_i) and weight term (m_i)

2. Angular acceleration term ($\dot{\omega}_i$)

3. Coordinates of mass centers $[(x_i \; y_i)]$

4. Linear acceleration of each link $\ddot{x}_i \; and \; \ddot{y}_i$

Calculation of terms 1-3 are direct forward but calculation of linear acceleration terms are complex and need to be adopt an iteration method.

6.2.1   Calculation of inertia term

The inertia term is depending on the robot link type. In this research it is assumed that the links are made out of slender bars. The equation used to calculate the inertia term as,

$$\frac{1}{12} mL^2$$

Where m -mass of the link

　　　L - length of the link

For this model it is also assumed as,

$\ldots = L_4$, $L_2 = L_5$

$m_1 = m_4$, $m_2 = m_3$

Therefore, I_1, I_2, I_3, I_4 can be calculated as follows;

$I_1 = 1/12\ m_1 L_1^2$

$I_2 = 1/12\ \ m_2\ L_2^2\ and$　　　　　　　　　　　　　　　　　　　　　(6.6)

$I_3 = I_3$

$I_4 = I_4$

Where, $m_1 \ldots m_4$ and $L_1 \ldots L_4$ are the masses and lengths of each link respectively.

6.2.2　Calculation of angular acceleration terms (ω)

For chapter 3 and 5 we derived equations for joint angles $\theta_1, \theta_2, \theta_3, \theta_5, \theta_6$ in equations (3.13) (3.8) (3.14) (5.5) (5.9)　these equations are in Cartesian domain that is it represent any angle respect to swing leg movement. The angular acceleration can be found by 2nd derivative of each equation. But there is a problem arising since we derived joint angle equations in Cartesian plane. It is impossible to obtain 2nd derivatives with respect to time if joint angle equations are in Cartesian domain. Therefore, we need to convert it to time domain. To convert this to time domain fifth order polynomial is used. The advantage of using this fifth-order polynomial is to ensure smooth functioning of joint angle variation. The fifth-order polynomial as-

$$q(t) = a_0 + a_1(t) + a_2(t)^2 + a_3(t)^3 + a_4(t)^4 + a_5(t)^5 \qquad (6.7)$$

Where $a_1, a_2, a_3, a_4\ and\ a_5$ are the coefficients, whose values are determined using different values of joint angles at different intervals of time cycle.

The assumed velocity variation with time is shown in Figure 6.2. This type of velocity profile has been selected to minimize jerks at the beginning and the end of the swinging foot.

The coefficients $a_1, a_2, a_3, a_4\ and\ a_5$ are found using following constrains in order to satisfy the velocity profile.

At $t = 0$ initial angular position

At $t = t_3$ final angular position

At $t = 0$ Initial angular velocity

At $t = t_3$ final angular velocity

At $t = t_1$ initial angular acceleration

At $t = t_2$ final angular acceleration
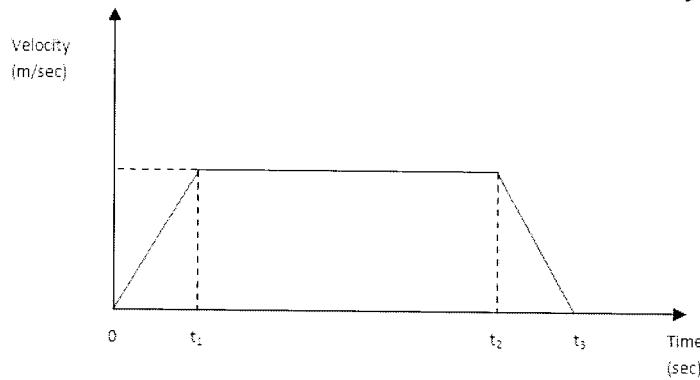
Figure 6.2: The velocity distribution of swing leg

The angular acceleration at any instant can be found out by derivation of the joint angle polynomial.

Therefore,

$$\alpha = 2a_2 + 6a_3 t + 12a_4 t^2 + 20a_5 t^3$$

Then using this equation $\ddot{\theta}_1(t), \ddot{\theta}_2(t), \ddot{\theta}_5(t)$ and $\ddot{\theta}_6(t)$ can be obtained. These are the angular accelerations of each link ($\dot{\omega}_1, \dot{\omega}_2, \dot{\omega}_3, \dot{\omega}_4$)

6.2.3 Finding of mass center coordinates

The mass centre coordinates has been derived using geometric relationships of links. The Fig. 6.3 shows the mass centre of each link and relevant coordinates.
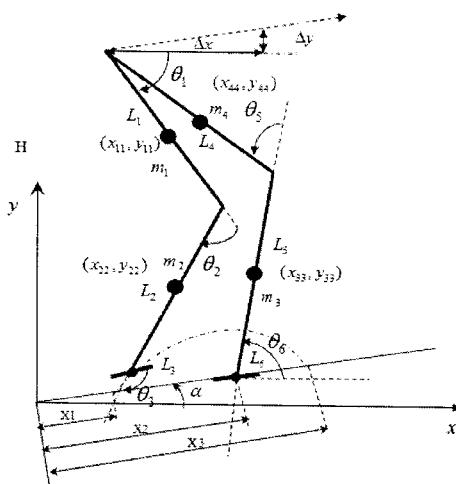
Figure 6.3: Mass Centre coordinats of each link

$m_1 = m_4$, $m_2 = m_3$ and $L_1 = L_4$, $L_2 = L_5$

$$x_1 = x_1 \cos\alpha + \Delta x + 0.5L_1 \cos\theta_1$$
$$y_1 = y + 0.5L_1 \sin\theta_1 + L_2 \sin[\pi - (\theta_1 + \theta_2)] \tag{6.8}$$

$$x_2 = x + 0.5L_2 \cos[\pi - (\theta_1 + \theta_2)]$$
$$y_2 = y + 0.5L_2 \sin[\pi - (\theta_1 + \theta_2)] \tag{6.9}$$

$$x_3 = x_2 \cos\alpha + 0.5L_2 \cos\theta_6$$
$$y_3 = x_2 \sin\alpha + 0.5L_2 \sin\theta_6 \tag{6.10}$$

$$x_4 = \Delta x + 0.5L_1 \cos[\pi - (\theta_5 + \theta_6)] + x_1 \cos\alpha$$
$$y_4 = x_2 \sin\alpha + L_2 \sin\theta_6 + 0.5L_1 \sin[\pi - (\theta_5 + \theta_6)] \tag{6.11}$$

41

6.3 Calculation of Individual link accelerations

There is no direct approach to find linear accelerations of links. In this model, all links are subjected to combine linear and angular motions. The acceleration of one link depends on the motion of the neighboring link. Therefore, an iteration method is preferred to solve this problem.

To solve this problem the Newton Euler Recursive iteration [18] is used.

6.3.1 Newton Euler Formulation

The Newton Euler (NE) formulation is based on the Newton's second law and d' Alembert principle. The balance of all forces acting on a link of the manipulator leads to a set of equations, whose structure allows a recursive solution. A forward recursion, which describes the kinematic relations of a moving coordinate frame, is performed for propagating velocities and accelerations, followed by a backward recursion for propagating forces and moments, Initially, it is assumed that the position, velocity, and acceleration of each joint, $(q, \dot{q}, \ddot{q})$ are known. The joint torques required to cause these time dependent motions to realize a trajectory are computed using the recursive NE dynamic equations of motion. To understand the Newton-Euler formulation, some basic concepts of kinematics are reviewed first.

The mass distribution of a link is completely characterized by the location of the centre of mass and the inertia tensor of the link. The forces or torques required for moving the links, and accelerating or decelerating them, are a function of the mass distribution and inertia tensor of the links.
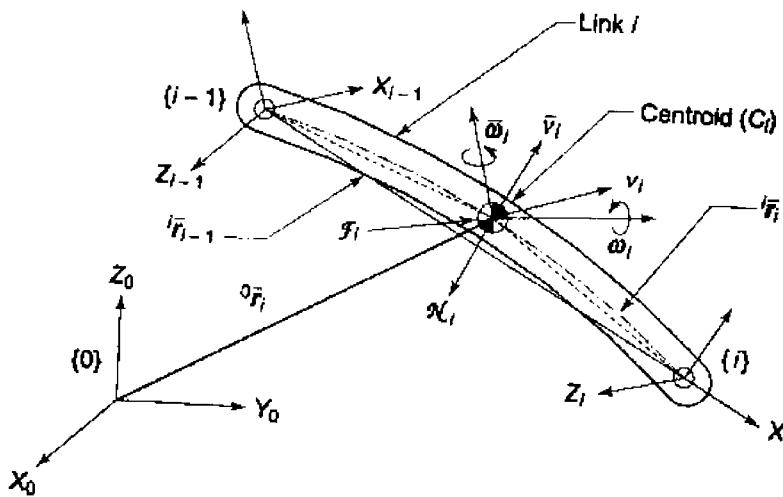

Figure 6.4: The Geometry and Kinematics of Link i for Newton Euler Formulation

Consider the rigid link i of the manipulator kinematic chain connected between joints i and $(i+1)$. The frames at the two ends are frame $\{i-1\}$ and frame $\{i\}$ as shown in Figure

42

(o 3) with reference to inertial frame $\{0\}$. The centre of mass of the link is C_i and the parameters listed below characterize the geometry and kinematics.

r	=	position vector of C_i from frame $\{i-1\}$,
c	=	position vector of C_i from frame $\{i\}$,
m	=	mass of link,
I	=	inertia tensor of link with respect to a frame $\{C_i\}$ whose origin is located at the centre of mass of the link C_i and orientation of frame $\{C_i\}$ is same as the orientation of the base frame $\{0\}$,
v	=	linear velocity of centre of mass of link
	=	linear acceleration of centre of mass,
ω	=	angular velocity of link,
ω	=	angular acceleration of link.
F	=	total external force acting at the centre of mass of link
N	=	total external moment acting on link at the centre of mass of link

The translational motion of the link in terms of the balance of forces is described by the *Newton's equation*. The force F_i, acting at the centre of mass of the link is given by

$$F = m_i \dot{\bar{v}}_i \qquad (6.12)$$

Where $\bar{v}_i$ is the linear acceleration of the link.

The Euler equation for the rotational motion of the link describes the moment balance about the centre of mass of the link. The angular velocity of the link ω_i and the moment of inertia tensor I_i relate to the total moment N_i acting on link as

$$N = \frac{d}{dt}(I_i \omega_i) = I_i \dot{\omega}_i + \omega_i \times (I_i \omega_i) \qquad (6.13)$$

Where the second term is the gyroscopic torque induced by the dependence of I_i on link's orientation with respect to base frame.

Equations (6.12) and (6.13) are the Newton-Euler equations that are recursively applied to compute the inertia force and torque acting at the centre of mass of each link of the manipulator.

In this case Newton's formula is enough because we need linear accelerations only. Euler equation formulates angular accelerations and is obtained using a fifth-order polynomial in section 6.2.2.

6.3.2 Kinematics of links

The kinematic relationship of the above moving-rotating links with respect to the base coordinate system is first described as a set of mathematical equations that needs to find accelerations. Two adjacent links i and $(i-1)$, forming the joint i are shown in Figure (6.5). The orthogonal coordinate frames are established with frame $\{0\}$ as the base coordinate frame; frame *frame* $\{i-1\}$ at joint i attached to link $(i-1)$ with point B as the origin, and frame (i) at joint $(i+1)$ attached to link i with origin D. The origin D and origin B are located by position vectors ^0D_i and $^0D_{i-1}$ with respect to the base frame $\{0\}$, respectively, and the position vector $^{i-1}D_i$ locates the origin D from the origin B with respect to the base coordinate system.
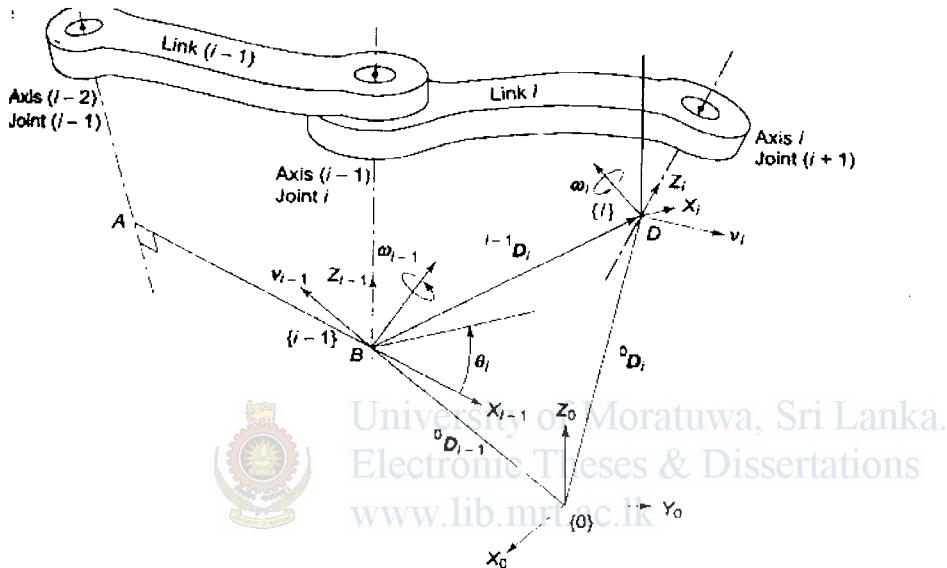
Figure 6.5: Characterization of two adjutant links forming the joint i for NE formulation

Let the linear and angular velocities of frame $\{i-1\}$, with respect to the base frame $\{0\}$, be v_{i-1} and ω_{i-1}, respectively, and ω_i be the angular velocity of frame $\{i\}$ with respect to the base frame $\{0\}$. Let $^{i-1}\omega_i$ be the relative angular velocity of frame i with respect to frame $\{i-1\}$ referred to base frame $\{0\}$. *Note that superscript '0' is omitted for quantities expressed in the base frame $\{0\}$.*

The linear velocity v_i of the frame (i) with respect to $\{o\}$ as

$$v_i = v_{i-1} + {}^{i-1}\dot{D}_i + \omega_{i-1} \times {}^{i-1}D_i \tag{6.14}$$

Where $^{i-1}\dot{D}_i$ denotes the velocity of frame $\{i\}$ with respect to the origin of frame $\{i-1\}$ expressed in base frame $\{0\}$.

44

If joint i is prismatic, link i travels in the direction of axes z_{i-1} with a linear joint velocity $\dot{d}_i$ relative to link $(i-1)$, that is, $^{i-1}\dot{D}_i = \hat{z}_{i-1}\dot{d}_i$, with $\hat{z}_{i-1}$ as the unit vector along z_{i-1} axis. The angular velocity of prismatic link i is same as that of link, that is $\omega_{i-1} = \omega_i$. Similarly, if the joint is revolute, the link i has an angular motion about the z_{i-1} axis with the angular velocity $\hat{z}_{i-1}\dot{\theta}_i$ and zero linear velocity, that is $^{i-1}\dot{D}_i = 0$

Substituting these linear velocities in equation (7.14), the linear velocity of link i with respect to reference frame is

$$v_i = \begin{cases} v_{i-1} + \hat{z}_{i-1}\dot{d}_i + \omega_i \times {}^{i-1}D_i & \textit{for prismatic joint} \\ v_{i-1} + \omega_i \times {}^{i-1}D_i & \textit{for revolute joint} \end{cases} \qquad (6.15)$$

The linear velocity is associated with a point and angular velocity is associated with a body. Hence, v_i, the linear velocity of the link $\{i\}$, and the angular velocity of the frame (i) is the velocity of the origin of the frame (i), ω_i is the angular velocity of the whole link i.

6.3.3 Link accelerations

In 6.3.2 n^{th} equation for linear velocity for a link is derived. But, to calculate ZMP it is needed to find link accelerations at its mass centers. Therefore, the link acceleration can be obtained by differentiating equation (6.15) with respect to time as:

$$\dot{v}_i = \dot{v}_{i-1} + \dot{\omega}_i \times {}^{i-1}D_i + \omega_i \times (\omega_i \times {}^{i-1}D_i) \qquad (6.16)$$

This is the linear acceleration of the link at its origin, but for ZMP computation it is needed to find linear acceleration at its mass center and it can be obtained as,
$$v = v_i + \omega_i {}^{i}r_i$$

$$\dot{v} = \dot{v}_i + \dot{\omega}_i \times {}^{i}\bar{r}_i + \omega_i \times (\omega_i \times {}^{i}\bar{r}_i) \qquad (6.17)$$

Where ${}^{i}\bar{r}_i$ is the position vector of centre of mass of link i with respect to base frame [0]

6.3.4 Recursive Newton Euler Formulation

The recursive formulation of dynamic equations based on NE equations is now carried out from the above kinematic information of each link. In the recursive formulation the serial open kinemtic chain structure of a manipulator is exploited. The NE formulation requires

45

two passes over the links of the manipulator, one for computing the velocities and accelerations of the links and, second, to compute joint forces and torques, as shown in Figure (6.6)
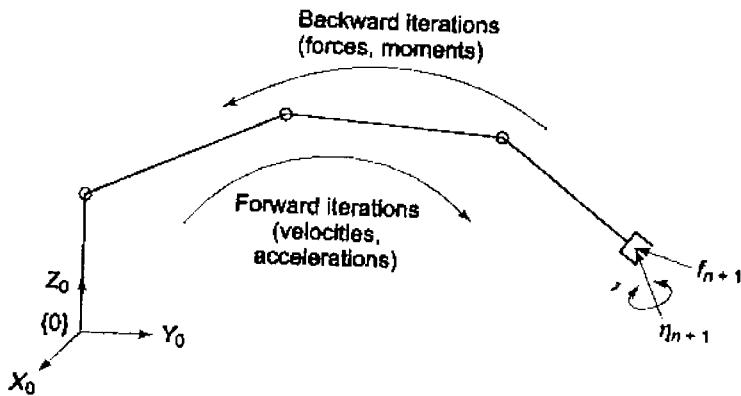

Figure 6.6: Two-pass recursive Newton Euler Formulation of dynamic equations

The *forward iteration or outward iteration* is carried out to compute the velocities and accelerations of each link recursively, starting at the base and propagating forward to the end-effector. The boundary conditions are base velocity, linear and angular, which are zero, (if the base is stationary) and the boundary acceleration is the gravitational acceleration.

In the backward or inward iteration, the forces and moments acting on each link are computed using the Newton's and Euler's equations.

6.3.5 Forward iteration

In the equations for velocity and acceleration, equations (6.15), (6.16) and (6.17), all the physical parameters are referenced to the base frame{0}. Because the parameters referred to the base frame change, as the manipulator is moving, the computations are complex. The computations are much simplified by referring all velocities, accelerations, inertia tensors, and location of centre of mass of each link to their own link-coordinate frames. The reference to link frame {i} results in constant inertia tensor I_i and constant vectors appear in the equations, simplifying the numerical computations. The change of frames is accomplished by using the 3x3 rotational transformation matrices, which give the kinematic relationship between the links.

The 3 x 3 rotation matrix $^{i-1}R_i$ transforms rotation of any vector with reference to frame {i} to the frame $\{i-1\}$. The rotation matrix $^{i-1}R_i$ is the upper left 3 x 3 sub-mart of $^{i-1}T_i$. That is

$$^{i-1}T_i = \begin{bmatrix} C\theta_i & -S\theta_i C\alpha_i & S\theta_i S\alpha_i & a_i C\theta_i \\ S\theta_i & C\theta_i C\alpha_i & -C\theta_i S\alpha_i & a_i S\theta_i \\ 0 & S\alpha_i & C\alpha_i & d_i \\ 0 & 0 & 0 & 1 \end{bmatrix} = \begin{bmatrix} ^{i-1}R_i & ^{i-1}D_i \\ 0\,0\,0 & 1 \end{bmatrix} \tag{6.19}$$

with $^{i-1}R_i = \begin{bmatrix} C\theta_i & -S\theta_i C\alpha_i & S\theta_i S\alpha_i \\ S\theta_i & C\theta_i C\alpha_i & -C\theta_i S\alpha_i \\ 0 & S\alpha_i & C\alpha_i \end{bmatrix}$; and $\begin{bmatrix} a_i C\theta_i \\ a_i S\theta_i \\ d_i \end{bmatrix}$ It can be shown that from basic robotics theory,

$$(^iR_i)^{-1} = {}^iR_{i-1} = (^{i-1}R_i)^T \tag{6.20}$$

Thus, using the rotational transformation matrices, it is possible to express the vectors related to link i with respect to link frame {i} instead of base frame {0}. This gives constant vectors instead of variable vectors, simplifying the numerical computations. Applying this, the velocity and acceleration relationships of equations (6.16), (6.17) are modified for the outward iteration as below. All the variables in these equations are now referred to their own frame.

$$^iR_{i-1}\,{}^{i-1}\dot{v}_{i-1} + {}^i\dot{\omega}_i \times (^iR_0\,{}^{i-1}D_i) + {}^i\omega_i\left[{}^i\omega_i \times (^iR_0\,{}^{i-1}D_i)\right] \tag{6.21}$$

The linear accelerations of the centre of mass is given by

$$^i\dot{v}_i + {}^i\omega_i \times {}^i\bar{r}_i + {}^i\omega_i \times (^i\omega_i \times {}^i\bar{r}_i) \tag{6.22}$$

The matrix products $\left(^iR_0\,{}^{i-1}D_i\right)$ in equation (6.21) are simplified, using equation (6.19) and (6.20), to yield

$$^iR_0\,{}^{i-1}D_i = \begin{bmatrix} C_1 & S_i & 0 \\ -S_i C\alpha_i & C_i C\alpha_i & S\alpha_i \\ S_i S\alpha_i & -C_i C\alpha_i & C\alpha_i \end{bmatrix} \begin{bmatrix} a_i C_i \\ a_i S_i \\ d_i \end{bmatrix} = \begin{bmatrix} a_i \\ d_i S\alpha_i \\ d_i C\alpha_i \end{bmatrix} \tag{6.23}$$

With $C_i = C\theta_i = \cos\theta_i$ and $S_i = S\theta_i = \sin\theta_i$

47

Equations (6.21) to (6.23) give forward Newton Euler equations. The forward iteration starts at the base, that is $i = 0$. The initial conditions for forward NE recursion for a fixed (inertial) base of manipulator are

$$\dot{\omega}_0 = 0$$

$$v_0 = 0$$

$$\omega_0 = 0$$

$$\dot{\omega}_0 = 0$$

The effect of gravity can be included by considering the linear accelerations of the base frame as

$$\dot{v}_0 = g = \begin{bmatrix} g_x & g_y & g_z \end{bmatrix}^T$$

The gravity loading on each link is then automatically propagated through the links by the forward recursion.

6.4 Application of N-E Recursive iteration to biped robot

To apply the forward iteration to biped robot lower body it is needed to separate the robot body as

(1) Swing Leg

(2) Stance Leg

### 6.4.1 Newton Euler Forward Iteration for Swing Leg
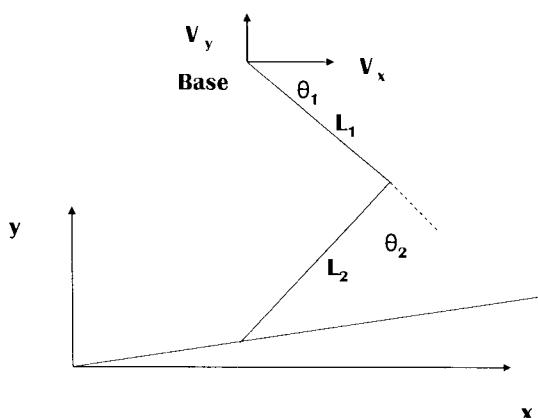
Figure 6.7: Initial position of the swing leg

Let us consider the swing leg, as a serial manipulator and its hip as the base. In this case the base of the manipulator is not fixed, as described in previous chapter in one gait cycle hip is moved by half of step length. In previous derivation initial conditions stated as:

$$v_0 = {}^0\dot{v}_0 = 0$$

But, in this case,

$v_0 \neq 0$ *and* ${}^0\dot{v}_0 \neq 0$ *and* initial condition as selected below:

$${}^0v_0 = \begin{bmatrix} v_x \\ v_y \\ 0 \end{bmatrix}; {}^0\omega_0 = {}^0\omega_0 = {}^0\dot{\omega}_0 = 0$$

Where v_x *and* v_y -initial velocity of the hip in x and y direction respectively

$$\therefore {}^0\dot{V}_0 = \begin{bmatrix} \dot{v}_x \\ (\dot{v}_y - g) \\ 0 \end{bmatrix}$$

For iteration following terms are also required,

$${}^iR_{i-1} = \begin{bmatrix} c_i & s_i & 0 \\ -s_i & c_i & 0 \\ 0 & 0 & 1 \end{bmatrix}$$

$${}^2R_0 = \begin{bmatrix} c_{12} & s_{12} & 0 \\ -s_{12} & c_{12} & 0 \\ 0 & 0 & 1 \end{bmatrix}$$

Using the equation (6.23),

$$^1R_0{}^0D_1 = \begin{bmatrix} a_1 \\ d_1 s\alpha_1 \\ d_1 c\alpha_1 \end{bmatrix} = \begin{bmatrix} L_1 \\ 0 \\ 0 \end{bmatrix}$$

Where L_1 and L_2 are the links lengths of swing leg.

$$^2R_0{}^1D_2 = \begin{bmatrix} L_2 \\ 0 \\ 0 \end{bmatrix}$$

Iteration start - $i = 1$

Using the equation (6.21) and substituting $i = 1$ we can get,

$$\dot{v}_1 = {}^1R_0 \; {}^0\dot{v}_0 + {}^1\omega_1 \times {}^1R_0{}^0D_1 + {}^1\omega_1 \times [{}^1\omega_1 \times ({}^1R_0{}^0D_1]$$ (6.24)

By substituting the above terms and initial conditions to the equation (6.24),

$$\dot{v}_1 = \begin{bmatrix} c_1 & s_1 & 0 \\ -s_1 & c_1 & 0 \\ 0 & 0 & 1 \end{bmatrix} \begin{bmatrix} \dot{v}_x \\ (\dot{v}_y - g) \\ 0 \end{bmatrix} + \begin{bmatrix} 0 \\ 0 \\ 1 \end{bmatrix} \ddot{\theta} \times \begin{bmatrix} L_1 \\ 0 \\ 0 \end{bmatrix} + \begin{bmatrix} 0 \\ 0 \\ 1 \end{bmatrix} \dot{\theta}_1 \times \left\{ \begin{bmatrix} 0 \\ 0 \\ 1 \end{bmatrix} \dot{\theta}_1 \times \begin{bmatrix} L_1 \\ 0 \\ 0 \end{bmatrix} \right\}$$

By simplifying we can end up,

$$^1\dot{v}_1 = \begin{bmatrix} \dot{v}_x C_1 + (\dot{v}_y - g)s_1 - L\dot{\theta}_1^2 \\ \dot{v}_x S_1 + (\dot{v}_y - g)C_1 + L\ddot{\theta}_1 \\ 0 \end{bmatrix} = \begin{bmatrix} \dot{v}_{1x} \\ \dot{v}_{1y} \\ 0 \end{bmatrix}$$ (6.25)

This is the acceleration at the origin of the link, but we need mass center acceleration, is given by using the equation (6.22)

$$
{}^1v_1 = \dot{v}_1 + {}^1\omega_1 \times {}^1\bar{r}_1 + {}^1\omega_1 \times ({}^1\omega_1 \times {}^1\bar{r}_1)
$$

$$
= \begin{bmatrix} \cdot \\ \cdot \\ 0 \end{bmatrix} + \begin{bmatrix} 0 \\ 0 \\ 1 \end{bmatrix}\ddot{\theta}_1 \times \begin{bmatrix} -1/2L_1 \\ 0 \\ 0 \end{bmatrix} + \begin{bmatrix} 0 \\ 0 \\ 1 \end{bmatrix}\dot{\theta}_1 \times \left\{ \begin{bmatrix} 0 \\ 0 \\ 1 \end{bmatrix}\dot{\theta} \times \begin{bmatrix} -L_1/2 \\ 0 \\ 0 \end{bmatrix} \right\}
$$

$$
\begin{bmatrix} \cdot_1 + (\dot{v}_y - g)S_1 - 1/2L_1\dot{\theta}_1^2 \\ \cdot \cdot_1 + (\dot{v}_y - g)C_1 + 1/2L_1\dot{\theta}_1 \\ 0 \end{bmatrix} = \begin{bmatrix} \ddot{x}_1 \\ \ddot{y}_1 \\ \ddot{z}_1 \end{bmatrix} \tag{6.26}
$$

Where $\ddot{x}_1$ *and* $\ddot{y}_1$ are the linear acceleration of link 1 in x and y direction respectively

To find linear accelerations for link-2 we need to continue the iteration, substituting $i = 2$. Recalling, equation (6.21) and using the equation (6.26) we can get
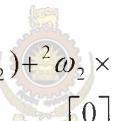
I

$$
= {}^2R_1\,{}^1\dot{v}_1 + {}^2\dot{\omega}_2 \times ({}^2R_0\,{}^1D_2) + {}^2\omega_2 \times \left[{}^2\omega_2 \times ({}^2R_0\,{}^1D_2) \right] \tag{6.27}
$$

$$
and\quad {}^2\omega_2 = \begin{bmatrix} 0 \\ 0 \\ 1 \end{bmatrix}(\dot{\theta}_1 + \dot{\theta}_2);\quad {}^2\dot{\omega}_2 = \begin{bmatrix} 0 \\ 0 \\ 1 \end{bmatrix}(\ddot{\theta}_1 + \ddot{\theta}_2)
$$

$$
R = \begin{bmatrix} C_2 & S_2 & 0 \\ -S_2 & C_2 & 0 \\ 0 & 0 & 1 \end{bmatrix}
$$

$$
= \begin{bmatrix} c_2 & s_2 & 0 \\ -s2 & c_2 & 0 \\ 0 & 0 & 1 \end{bmatrix}\begin{bmatrix} \dot{v}_{1x} \\ (\dot{v}_{1y}) \\ 0 \end{bmatrix} + \begin{bmatrix} 0 \\ 0 \\ 1 \end{bmatrix}(\ddot{\theta}_1 + \ddot{\theta}_2 \times \begin{bmatrix} L_2 \\ 0 \\ 0 \end{bmatrix} + \begin{bmatrix} 0 \\ 0 \\ 1 \end{bmatrix}(\dot{\theta}_2 + \dot{\theta}_1) \times \left\{ \begin{bmatrix} 0 \\ 0 \\ 1 \end{bmatrix}(\dot{\theta}_1 + \dot{\theta}_2) \times \begin{bmatrix} L_2 \\ 0 \\ 0 \end{bmatrix} \right\}
$$

By simplification to equation

$$
v_2 = \begin{bmatrix} \dot{v}_{1x}C_2 + \dot{v}_{1y}S_2 - L_2(\dot{\theta}_1 + \dot{\theta}_2)^2 \\ -\dot{v}_{1x}S_2 + \dot{v}_{1y}C_2 + L_2(\ddot{\theta}_1 + \ddot{\theta}_2) \\ 0 \end{bmatrix}
$$

These are the accelerations at the origin of the link 2. But, we need accelerations at mass centre of the link 2.

$$v_2 = {}^2\dot{v}_2 + {}^2\dot{\omega}_2 \times {}^2\bar{r}_2 + {}^2\omega_2 \times \left[{}^2\omega_2 \times {}^2\bar{r}_2\right]$$

By substituting ${}^2\bar{r}_2 = \begin{bmatrix} -L_2/2 \\ 0 \\ 0 \end{bmatrix}$ and simplifying

$$\ddot{r}_2 = \begin{bmatrix} \dot{v}_{1x} C_2 + \dot{v}_{1y} S_2 - L_2(\dot{\theta}_1 + \dot{\theta}_2)^2 + 1/2\, L_2(\dot{\theta}_1 + \dot{\theta}_2)^2 \\ -\dot{v}_{1x} S_2 + \dot{v}_{1y}\ C_2 + L_2(\ddot{\theta}_1 + \ddot{\theta}_2) - 1/2\, L_2(\ddot{\theta}_1 + \ddot{\theta}_2) \\ 0 \end{bmatrix} = \begin{bmatrix} \ddot{x}_2 \\ \ddot{y}_2 \\ \ddot{z}_2 \end{bmatrix} \qquad (6.28)$$

$\ddot{x}_2, \ddot{y}_2$ are the linear accelerations of link 2 of the swing leg at its mass centre along X and Y directions.

Iteration stopped,

Final Results for linear accelerations of swing leg

$$\ddot{x}_1 = \dot{v}_x C_1 + (\dot{v}_y - g)S_1 - 1/2 L_1\dot{\theta}_1^2$$

$$\ddot{y}_1 = \dot{v}_x S_1 + (\dot{v}_y - g)C_1 - 1/2 L_1 \ddot{\theta}_1$$

$$\ddot{x}_2 = v_{1x}C_2 + \dot{v}_{1y} S_2 - 1/2 L_2(\dot{\theta}_1 + \dot{\theta}_2)^2$$

$$\ddot{y}_2 = -\dot{v}_{1x} S_2 + \dot{v}_{1y} C_2 + 1/2 L_2(\ddot{\theta}_1 + \ddot{\theta}_2)$$

$\dot{v}_x$ and $\dot{v}_y$ are the hip accelerations along x and y direction respectively and will be obtained in **stance leg velocity derivations.**

## 6.4.2 Newton Euler forward recursive iteration for stance leg
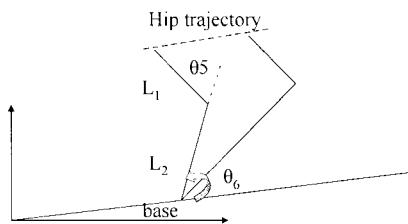
Figure 6.8: Initial and final position of the stance leg during one gait cycle

In this case the ankle of stance leg is considered as the base. This case differs from previous iteration due to stationary base (ankle). Therefore, the initial conditions for this iteration as,

$$^0\omega_0 = {}^0\dot{\omega}_0 = 0$$

$$= [0, -g \ 0]^T$$

Following terms are required to start the iteration

Using the equation (7.23) and $a_3 = L_2$ and $a_4 = L_1$
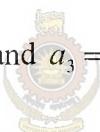
$$R_{} = \begin{bmatrix} C_{65} & S_{65} & 0 \\ -S_{65} & C_{65} & 0 \\ 0 & 0 & 1 \end{bmatrix}$$

$$R_{}{}^{i-1}D_i = \begin{bmatrix} a_i \\ d_i s\alpha_i \\ d_i c\alpha_i \end{bmatrix}$$

$$R_{}{}^2 D_3 = \begin{bmatrix} L_2 \\ 0 \\ 0 \end{bmatrix} \ and \ {}^4R_3.{}^3D_4 = \begin{bmatrix} L_1 \\ 0 \\ 0 \end{bmatrix}$$

$$\ ^iR_{i-1}\ {}^i\dot{v}_i + \dot{\omega}_i \times {}^iR_{i-1}\ {}^{i-1}D_i +{}^i\omega_i \times \left[{}^i\omega_i x({}^iR_{i-1}\ {}^{i-1}D_i) \right]$$

Iteration start,

$i =$

By substituting above terms and initial conditions we can obtain,

53

$$v_3 = {}^3R_2\,{}^3\dot{v}_3 + {}^3\dot{\omega}_3 \times {}^3R_2\,{}^2D_3 + {}^3\omega_3 \times \left[{}^3\omega_3 \times \left({}^3R_2\,{}^2D_3\right)\right] = \begin{bmatrix} c_6 & s_6 & 0 \\ -s_6 & c_6 & 0 \\ 0 & 0 & 1 \end{bmatrix}\begin{bmatrix} 0 \\ -g \\ 0 \end{bmatrix} + \begin{bmatrix} 0 \\ 0 \\ 1 \end{bmatrix}\ddot{\theta}_6 \times \begin{bmatrix} L_2 \\ 0 \\ 0 \end{bmatrix} +$$

$$\begin{bmatrix} 0 \\ 0 \\ 1 \end{bmatrix}\dot{\theta}_6 \times \left\{ \begin{bmatrix} 0 \\ 0 \\ 1 \end{bmatrix}\dot{\theta}_6 \times \begin{bmatrix} L_2 \\ 0 \\ 0 \end{bmatrix} \right\}$$

By simplifying

$$v_3 = \begin{bmatrix} -gs_6 - L_2\dot{\theta}_6^2 \\ -gc_6 + L_2\ddot{\theta}_6 \\ 0 \end{bmatrix}$$

This is the linear acceleration at the origin of the link. But, we need acceleration at the mass centre of the link.

Then the acceleration at mass centre of the link is given by in equation (6.22) as,

$$v_3 = {}^3\dot{v}_3 + {}^3\dot{\omega}_3 \times {}^3\bar{v}_3 + {}^3\omega_3 \times \left[{}^3\omega_3 \times {}^3\bar{r}_3\right]$$

By substituting and simplifying

$$v_3 = \begin{bmatrix} -gs_6 & -L_2\dot{\theta}_6^2 \\ -gc_6 & +L_2\ddot{\theta}_6 \\ 0 \end{bmatrix} ; = \begin{bmatrix} \ddot{x}_3 \\ \ddot{y}_3 \\ \ddot{z}_3 \end{bmatrix} \qquad (6.29)$$

These are the linear accelerations of link 3 of stance leg in the direction of x,y,z respectively

Iteration continues,
$i = 4$

$$v_4 = {}^4R_3\,{}^3\dot{v}_3 + {}^4\dot{\omega}_4 \times {}^4R_3\,{}^3D_4 + {}^4\omega_4 \times \left[{}^4\omega_4 \times \left({}^4R_3\,{}^3D_4\right)\right]$$

By substituting values,

54

$$\mathbf{v}_i = \begin{bmatrix} c_5 & +s_5 & 0 \\ -s_5 & c_5 & 0 \\ 0 & 0 & 1 \end{bmatrix} \begin{bmatrix} -gs_6 - L_2\theta_6^2 \\ -gc_6 + L_2\ddot{\theta}_6 \\ 0 \end{bmatrix} + \begin{bmatrix} 0 \\ 0 \\ 1 \end{bmatrix}(\ddot{\theta}_6 + \ddot{\theta}_5) \begin{bmatrix} L_1 \\ 0 \\ 0 \end{bmatrix} + \begin{bmatrix} 0 \\ 0 \\ 1 \end{bmatrix}(\dot{\theta}_6 + \dot{\theta}_5) \times \left\{ \begin{bmatrix} 0 \\ 0 \\ 1 \end{bmatrix}(\dot{\theta}_6 + \dot{\theta}_5) \times \begin{bmatrix} L_1 \\ 0 \\ 0 \end{bmatrix} \right\}$$

By simplifying

$$\mathbf{v}_i = \begin{bmatrix} L_2\ddot{\theta}_6 S_5 - L_2\dot{\theta}_6^2 C_5 - L_1\ddot{\theta}_6 - L_1\dot{\theta}_5^2 - 2L_1\dot{\theta}_6\dot{\theta}_5 - gS_{65} \\ L_2\ddot{\theta}_6 C_5 + L_1\ddot{\theta}_6 + L_1\ddot{\theta}_5 + L_2\dot{\theta}_6^2 S_5 - gC_{65} \\ 0 \end{bmatrix} ,$$

Where $S_5 = Sin\theta_5$, $C_5 = Cos\theta_5$, $C_{65} = Cos(\theta_6 + \theta_5)$ and $S\theta_{65} = Sin(\theta_6 + \theta_5)$

These are the linear accelerations of the end effector of the stance leg. In this case we consider the end effector being hip. Therefore, this is the linear acceleration of hip in x and y directions respectively. In swing leg forward iteration we consider the initial linear acceleration of hip as $\dot{v}_x$ and $\dot{v}_y$ as

$$\begin{bmatrix} \dot{v}_x \\ \dot{v}_y \\ \dot{v}_z \end{bmatrix} = \begin{bmatrix} L_2\ddot{\theta}_6 S_6 - L_2\dot{\theta}_6^2 c_5 - L_1\dot{\theta}_6^2 - L_1\dot{\theta}_5^2 - 2L_1\dot{\theta}_5\theta_6 - gs_{56} \\ L_2\ddot{\theta}_6 c_6 + L_1\ddot{\theta}_6 + L_1\ddot{\theta}_5 + L_2\dot{\theta}_6^2 S_5 - gc_{56} \\ 0 \end{bmatrix} \tag{6.30}$$

Let us take these accelerations as

$$\begin{bmatrix} \dot{v}_{4x} \\ \dot{v}_{4y} \\ \dot{v}_{4z} \end{bmatrix}$$

The accelerations at the mass centre of the link is calculated using

$$\dot{v}_i = {}^4\dot{v}_4 + {}^4\dot{\omega}_4 \times {}^4\bar{v}_4 + {}^4\omega_4 \times \left[{}^4\omega_4 \times {}^4\bar{v}_4 \right]$$

Substituting the values and simplifying

$$\begin{bmatrix} \ddot{x}_4 \\ \ddot{y}_4 \\ \ddot{z}_4 \end{bmatrix} = \begin{bmatrix} \dot{v}_{4x} + \dfrac{L_1}{2}(\dot{\theta}_5 + \dot{\theta}_6)^2 \\ \dot{v}_{4y} - \dfrac{L_1}{2}(\ddot{\theta}_5 + \ddot{\theta}_6) \\ 0 \end{bmatrix} \qquad (6.31)$$

6.5 Dynamic stability analysis for robot lower body

All the terms that need to be calculated ZMP, have now been derived. By using these equations, the ZMP can be obtained in different time intervals. The graph, ZMP vs time, can be obtained by using mathlab software.

Utilizing the Figure (6.11) the dynamic stability can be analyzed for lower body by considering dynamic balanced margin [2].

6.5.1 Dynamic balance margin

The dynamic balance margin (DBM) can be defined as below.

For single support phase
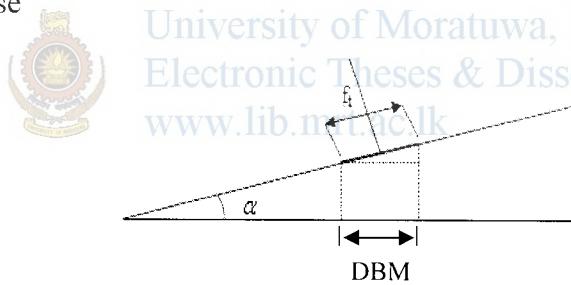
Figure 6.9: DBM for single support phase

Referring the figure (6.9) the DBM can be defined as $-(f_t \cos\alpha)/2$ and $(f_t \cos\alpha)/2)$ Therefore the requirement for robot to maintain dynamic stability in single support phase is

$-(f_t / 2 \cos\alpha)/2 \le ZMP \le (f_t \cos\alpha)/2$

Where, f_t is the foot length.

In single support phase, the ZMP can easily be moved to the outside of this margin. Therefore, much attention is needed on balancing in this phase. (since only one foot touches the ground)

In double support phase, the balance of the robot is not a critical problem as the ground is touched by both feet. The requirement for stability can be shown in Figure (6.10)
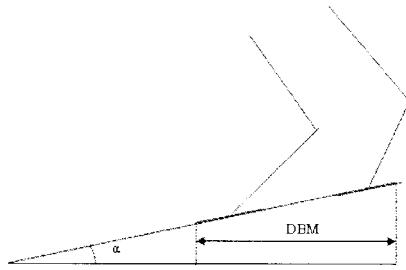

Figure 6.10: DBM for double support phase

The DBM for this case can be obtained as,

$$-f_t/2\cos\alpha) \le ZMP \le \left[(x_2 - x_1) + f_t/2\right]\cos\alpha$$

This is a large margin compared to DBM in single support phase.

6.5.2 Simulation result on stability - robot lower body

Utilizing the derived equations for ZMP and DBM, the variation of ZMP in one gait cycle can be plotted [22] as follows with the aid of mathlab software.

Figure 6.11 shows the variation of ZMP with respect to time of Robot's lower body, within one gait cycle. The table 6.1 introduced the selected physical parameters for simulation. The zone between the two red lines in Figure 6.11 is the dynamic balanced margin or DBM. If ZMP lies outside of this zone and within this area the robot is not dynamically balanced and is not capable to maintain it's stability and therefore, it falls on the ground. The blue line represents the variation of computed ZMP for lower body. The Figure 6.11 shows the designed robot's lower body which is unstable in whole gait cycle excluding the final stage.

Parameter	Value
Angle of Slope	5 °
L1	460 mm
L2	480 mm
m1	5 Kg
m2	5.2 Kg

**Table 6.1: Selected Physical Parameters for Lower Body Simulation**
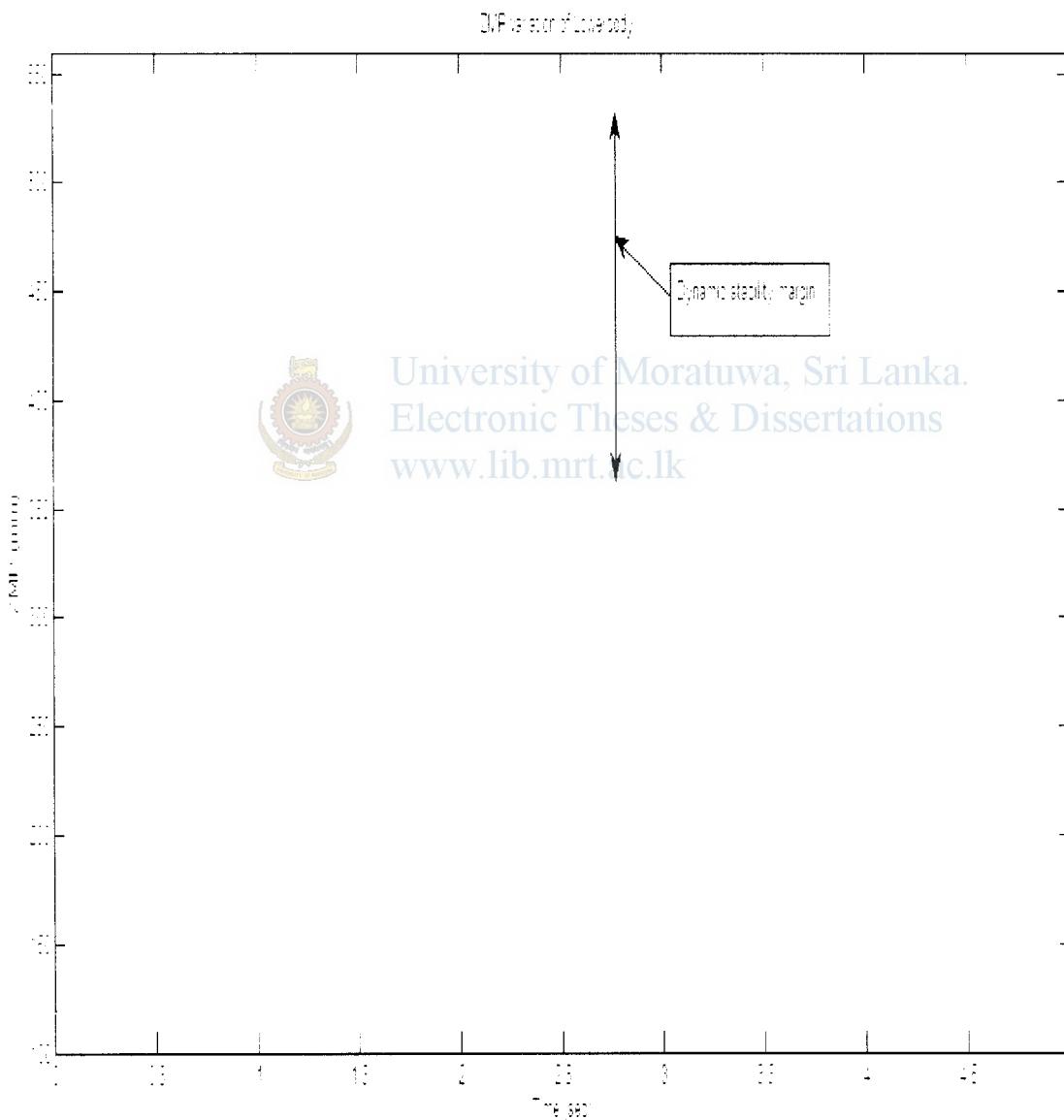
Figure 6.11: Variation of ZMP Vs Time of lower body for one gait cycle

ZMP Calculation After Adding Torso

7.1 Modification of ZMP

According to the chapter 6, the ZMP of the lower body of the robot is out of the DBM. That means the robot is unbalanced during the gait cycle. Therefore, it is needed to modify the robot structure to maintain its stability by improving ZMP.

7.1.1 Method for improving the ZMP

By using the following methods it can be seen that the ZMP can be improved.

  (i)   By adjusting link length
  (ii)   By adjusting link weight
  (iii)   By adjusting step length
  (iv)   By adjusting cycle time
  (v)   By adding of torso to lower body and adjusting torso angle

Considering the above methods, it can be seen that the last one is the most effective method to improve ZMP.

7.2 Calculation of improved ZMP

In the chapter 6, it is noted that the ZMP is calculated only for lower body of the robot by considering the total number of link is 4. After addition of the torso the number of link is increased to five. To calculate improved ZMP, the following additional terms are need to be calculated.

- Inertia term - I_5
- Torso mass centre coordinates - (x_5, y_5)

- Angular acceleration term - $\ddot{\theta}_7$
- Torso length and mass of the torso $(L_T), (m_T)$

- Linear accelerations of torso $\left(\ddot{x}_5, \ddot{y}_5 \right)$

The calculation of the above terms is same as previous, except calculation of the linear acceleration term

(a) Inertia term

Here also slender bar has been used for Torso and its inertia I_T is been given by $I_T = 1/12mL_1^2$,

(b) Angular acceleration term θ_7

This is the control parameter to maintain the stability of the robot. By controlling this angle the ZMP can be moved to a stable region when the robot can not maintain the stability.

The angular acceleration assumed to be small compared to the link accelerations, and also it is not practical to move the torso in each instant because the ZMP will vary in a wider margin.

(c) Torso link weight and torso link length L_T

Torso link length L_T and torso weight m_T are selectable and fixed values.

7.2.1 Calculation of Linear acceleration terms $\ddot{x}_5, \ddot{y}_5$

In chapter 6, the Newton Euler iteration continued up to $i = 4$ for stance leg. By assuming the torso is the 5th link of stance leg, the same iteration can be continued upto $i = 5$.
Iteration starts from i=5

$$^5\dot{v}_5 = {^5R_4}\ ^4\dot{v}_4 + {^5\dot{\omega}_5} \times ({^5R_0}\ ^4D_5) + {^5\omega_5} \times \left[{^5\omega_5} \times ({^5R_0}\ ^4D_5) \right] \tag{7.1}$$

$$^iR_0\ ^{i-1}D_i = \begin{bmatrix} a_i \\ d_i S\alpha_i \\ d_i C\alpha_i \end{bmatrix}$$

$$^{i-1}R_i = \begin{bmatrix} C\theta_i & -S\theta_i C\alpha_i & S\theta_i S\alpha_i \\ S\theta_i & C\theta_i C\alpha_i & -C\theta_i S\alpha_i \\ 0 & S\alpha_i & C\alpha_i \end{bmatrix}$$

By substituting $i = 5$

$$^4R_5 = \begin{bmatrix} \cos\theta_7 & -\sin\theta_7 & 0 \\ \sin\theta_7 & \cos\theta_7 & 0 \\ 0 & 0 & 1 \end{bmatrix}, {^5R_4} = \begin{bmatrix} \cos\theta_7 & \sin\theta_7 & 0 \\ -\sin\theta_7 & \cos\theta_7 & 0 \\ 0 & 0 & 1 \end{bmatrix}$$

Using equation (7.1) and $^5R_4$,

60

$$
{}^5\dot{v}_5 = \begin{bmatrix} C\theta_7 & -S\theta_7 & 0 \\ S\theta_7 & C\theta_7 & 0 \\ 0 & 0 & 1 \end{bmatrix}\begin{bmatrix} \dot{v}_{4x} \\ \dot{v}_{4y} \\ 0 \end{bmatrix} + \begin{bmatrix} 0 \\ 0 \\ 1 \end{bmatrix}(\ddot{\theta}_6 + \ddot{\theta}_5 + \ddot{\theta}_7)\times \begin{bmatrix} L_T \\ 0 \\ 0 \end{bmatrix}
$$

$$
+ \begin{bmatrix} 0 \\ 0 \\ 1 \end{bmatrix}(\dot{\theta}_6 + \dot{\theta}_5 + \dot{\theta}_7)\times \left\{ \begin{bmatrix} 0 \\ 0 \\ 1 \end{bmatrix}(\dot{\theta}_6 + \dot{\theta}_5 + \dot{\theta}_7)\times \begin{bmatrix} L_T \\ 0 \\ 0 \end{bmatrix} \right\}
$$

By simplifying,

$$
{}^5\dot{v}_5 = \begin{bmatrix} (\dot{v}_{4x}\cos\theta_7 - \dot{v}_{4y}\sin\theta_7) \\ (\dot{v}_{4x}\sin\theta_7 + \dot{v}_{4y}\cos\theta_7) \\ 0 \end{bmatrix} + \begin{bmatrix} -L_T(\dot{\theta}_6 + \dot{\theta}_5 + \dot{\theta}_7)^2 \\ 0 \\ 0 \end{bmatrix}
$$

$$
{}^5\dot{v}_5 = \begin{bmatrix} (\dot{v}_{4x}\cos\theta_7 - \dot{v}_{4y}\sin\theta_7 - L_T(\dot{\theta}_6 + \dot{\theta}_5 + \dot{\theta}_7)^2 \\ -(\dot{v}_{4x}\sin\theta_7 + \dot{v}_{4y}\cos\theta_7 + L_T(\ddot{\theta}_6 + \ddot{\theta}_5 + \ddot{\theta}_7) \\ 0 \end{bmatrix}
$$

These are the acceleration at the origin of the torso. But we need acceleration at the mass center of the torso. Using the equation (6.22) and substituting $i = 5$ we can get,

$$
{}^5\ddot{\vec{v}}_5 = \begin{bmatrix} \ddot{X}_5 \\ \ddot{Y}_5 \\ \ddot{Z}_5 \end{bmatrix} = \begin{bmatrix} \dot{v}_{5x} + L_T/2(\dot{\theta}_6 + \dot{\theta}_5 + \dot{\theta}_7)^2 \\ \dot{v}_{5y} - L_T/2(\ddot{\theta}_6 + \ddot{\theta}_5 + \ddot{\theta}_7) \\ 0 \end{bmatrix}
$$

$$
\ddot{X}_5 = \dot{v}_{4x}\sin\theta_7 - \dot{v}_{4y}\sin\theta_7 - 1/2 L_T(\dot{\theta}_6 + \dot{\theta}_5 + \dot{\theta}_7)^2 \tag{7.2}
$$

$$
\ddot{Y}_5 = \dot{v}_{4x}\sin\theta_5 + \dot{v}_{4y}\cos\theta_7 + 1/2 L_T(\ddot{\theta}_6 + \ddot{\theta}_5 + \ddot{\theta}_7) \tag{7.3}
$$

Where L_T is the length of the torso, and θ_5 is the torso angle with measuring from second link of the stance foot.

By substituting these terms to the original ZMP equation a very complex second order non linear differential equation can be obtained as,

$$ZMP = f\left(\theta_7, m_T, L_T\right)$$

The torso weight and torso length are selectable and fixed values. The only variable of this function is θ_7. Utilizing this function the optimum torso angle can be obtained to maintain the ZMP within the safe margin while walking the robot.

The variation of ZMP, selection of parameters and, control of torso angle to maintain dynamic stability can be obtained by simulating the model by using the mathlab software.

7.3 Stability Analysis from simulation results

The variables for this simulation are:

i.   Torso angle(θ_7)
ii.   Slope angle (α)
iii.   Step length ($x_2 - x_1$)
iv.   Mass of torso(M_T)
v.   Length of torso (L_T)
vi.   Step time (t)
vii.   Mass of links L_1 and L_2 (m_1 and m_2)

But, the torso angle is the only variable that can be varied over step time. Other parameters are selectable and fixed.

Parameter	Value
Angle of Slope	5 °
L1	460 mm
L2	480 mm
LT	800 mm
m1	5 Kg
m2	5.2 Kg
Step Length	700mm
mT	35 Kg

Table 7.1: Physical parameters for simulation 1

Figure 7.1: Variation of ZMP with torso angle at slope angle equal to 5 °

Parameter	Value
Angle of Slope	10 °
L1	460 mm
L2	480 mm
LT	800 mm
m1	5 Kg
m2	5.2 Kg
Step Length	700mm
mT	35 Kg

Table 7.2: Physical parameters for simulation 2


Figure 7.2: Variation of ZMP with torso angle at slope angle equal to 10 °

63

7.3.1 ZMP variation with slope angle

Parameter	Value
Angle of Slope	5 °
L1	460 mm
L2	480 mm
LT	800 mm
m1	5 Kg
m2	5.2 Kg
Step Length	700mm
mT	35 Kg

Table 7.1: Physical parameters for simulation 1
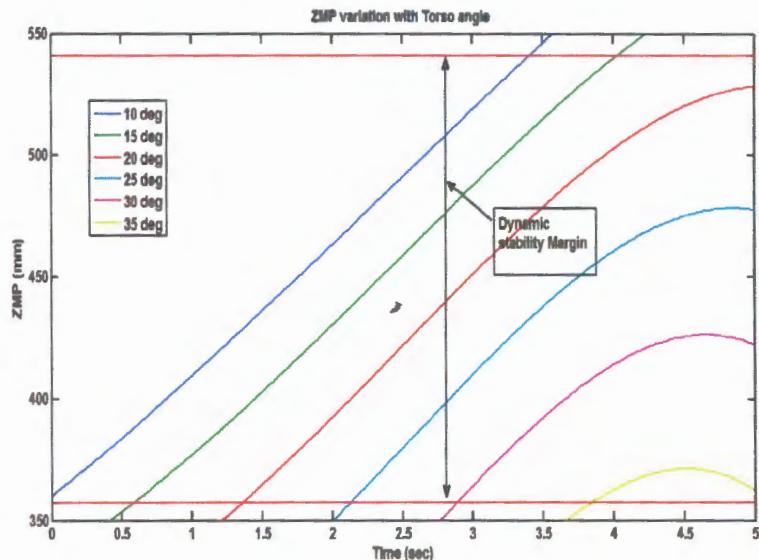
Figure 7.1: Variation of ZMP with torso angle at slope angle equal to 5 °

Parameter	Value
Angle of Slope	10 °
L1	460 mm
L2	480 mm
LT	800 mm
m1	5 Kg
m2	5.2 Kg
Step Length	700mm
mT	35 Kg

Table 7.2: Physical parameters for simulation 2

Figure 7.2: Variation of ZMP with torso angle at slope angle equal to 10 °

Parameter	Value
Angle of Slope	15°
L1	460 mm
L2	480 mm
L3	800 mm
m1	5 Kg
m2	5.2 Kg
Step Length	700mm
mT	35 Kg

Table 7.3: Physical parameters for simulation 3
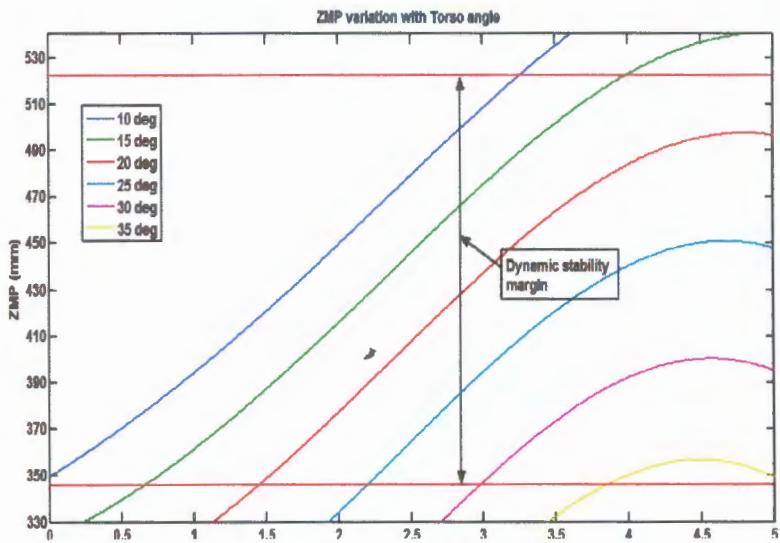

Figure 7.3: Variation of ZMP with torso angle at slope angle equal to 15°

Figure (7.1), (7.2), (7.3) show the ZMP variation with slope angle and, by utilizing these simulations it can be noted that the dynamic stability can be maintained by varying torso angle between 10-20 degrees in all three cases.

7.3.2 ZMP variation with step length

Parameter	Value
Angle of Slope	5°
L1	460 mm
L2	480 mm
m1	5 Kg
m2	5.2 Kg
Step Length	700mm
LT	35 Kg

Table 7.4: Physical parameters for simulation 4
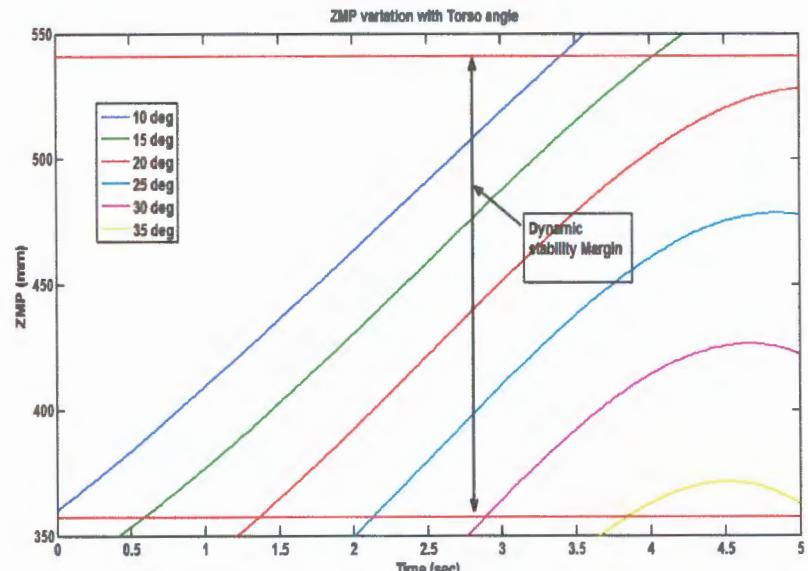
Figure 7.4: ZMP variation with torso angel when step length is 700mm

Parameter	Value
Angle of Slope	5 °
L1	460 mm
L2	480 mm
m1	5 Kg
m2	5.2 Kg
Step Length	350mm
LT	35 Kg

Table 7.5: Physical parameters for simulation 5
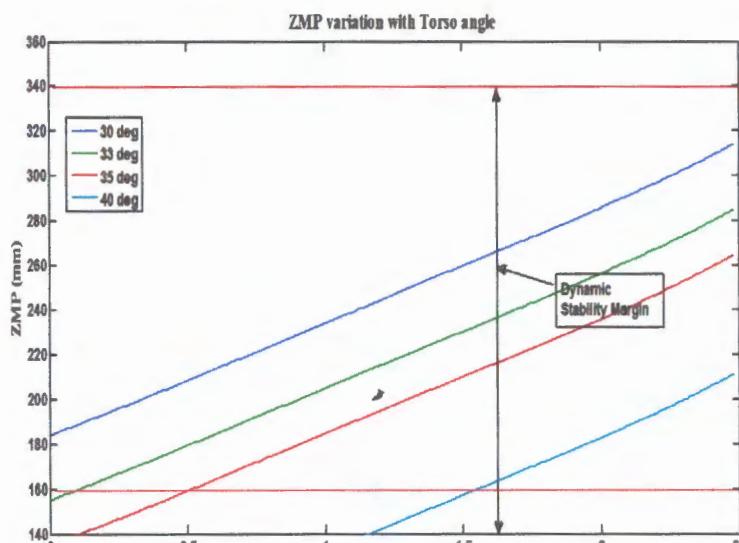
Figure 7.5: ZMP variation with torso angle when step length is 350mm

| Parameter	Value
Angle of Slope	5 °
L1	460 mm
L2	480 mm
m1	5 Kg
m2	5.2 Kg
Step Length	150mm
LT	35 Kg

Table 7.6: Physical parameters for simulation 6
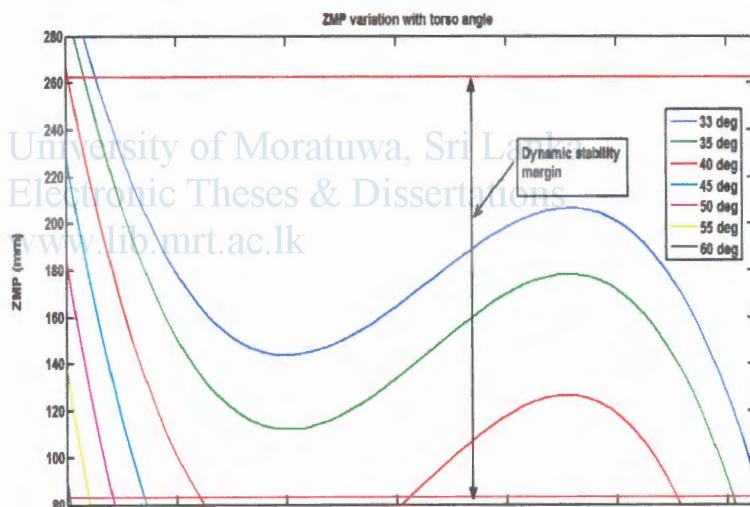
Figure 7.6: ZMP variation with torso angle when step length is 150mm

With the aid of Figure (7.4), (7.5), (7.6) it can be summarized the torso angle variation as:

1. At full step –Torso angle variation is 10-20 degree to maintain dynamic stability, maximum angle being 35 degrees.

2. At half step- Torso angle variation is 30-33 degrees to maintain dynamic stability. The maximum angle can be 40 degrees.

3. At quarter step- The torso angle can be varied between 33-40 degrees. The minimum torso angle can be 60 degrees.

7.3.3   ZMP variation with mass of torso

Parameter	Value
Angle of Slope	10 °
L1	460 mm
L2	480 mm
m1	5 Kg
m2	5.2 Kg
LT	850mm
Step Length	150mm
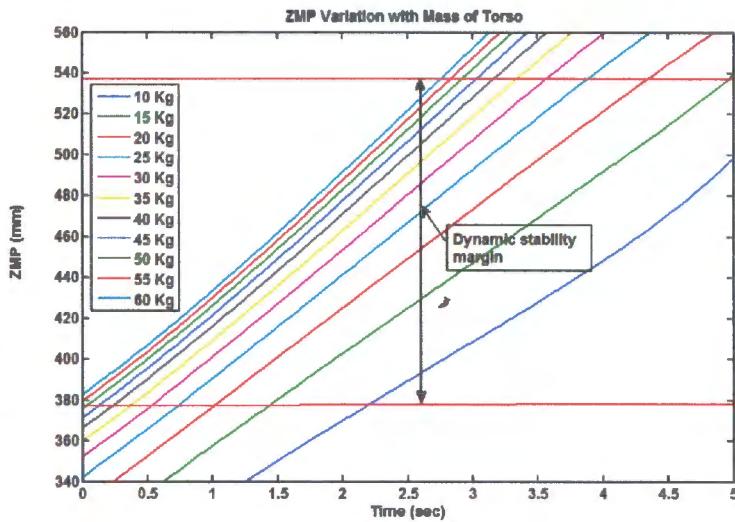
**Table 7.7: Physical parameters for simulation 7**

Figure7.7: Variation of ZMP with different values of torso weight

Figure (7.7) shows the ZMP variation with respect to different values of torso weight; when increasing the torso weight the dynamic stability is also improves. But, after a certain point, the increment of torso weight is not much affected to the dynamic stability

7.3.4   ZMP Variation with torso length

Parameter	Value
Angle of Slope	15 °
L1	460 mm
L2	480 mm
m1	5 Kg
m2	5.2 Kg
LT	850mm
Step Length	150mm
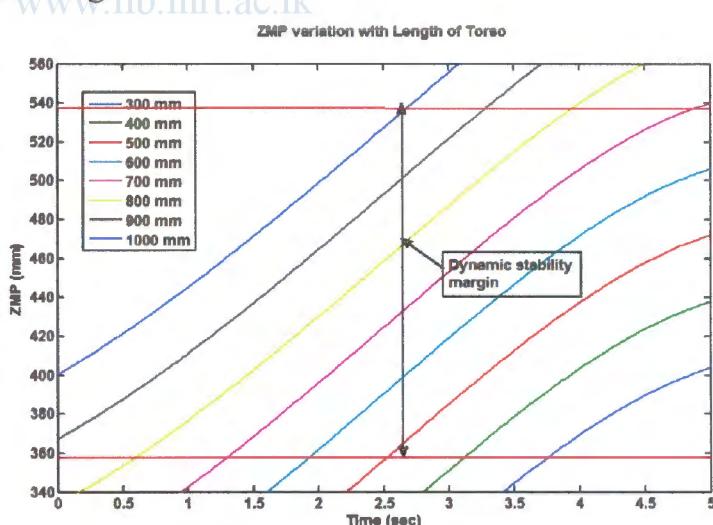
**Table 7.8: Physical parameters for simulation 8**

Figure 7.8: Variation of ZMP for different values of torso length

Figure (7.8) shows the variation of ZMP with torso length. The dynamic stability can be improved by increasing the torso length but, there are practical limitations.

7.3.5 Variation of ZMP with step time

Parameter	Value
Angle of Slope	5 °
L1	460 mm
L2	480 mm
m1	5 Kg
m2	5.2 Kg
LT	850mm
Step Length	700mm

Table 7.9: Physical parameters for simulation 9
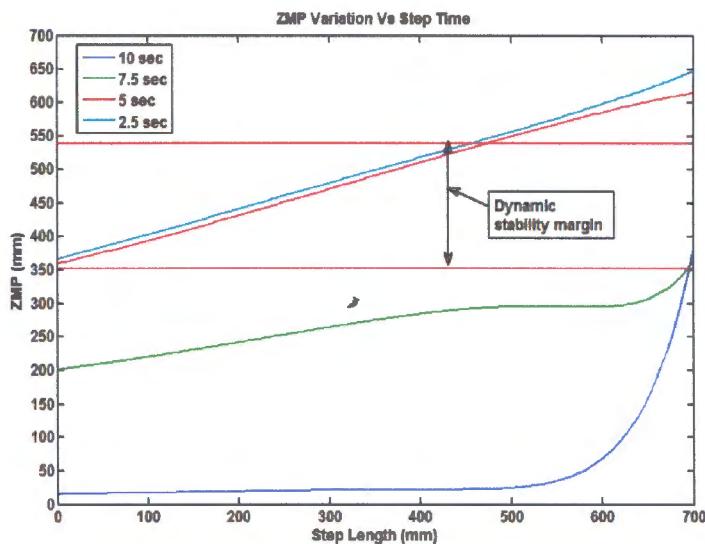

Figure 7.9: Variation of ZMP with different step time intervals

Figure (7.9) shows the variation of ZMP in different step time intervals. According to this simulation result, it can be noticed that the dynamic stability improves in fast walking.

7.3.6 ZMP variation with link length L_1 and L_2

Parameter	Value
Angle of Slope	5 °
m1	5 Kg
m2	5.2 Kg
LT	850mm
Step Length	700mm

**Table 7.10: Physical parameters for simulation 10**
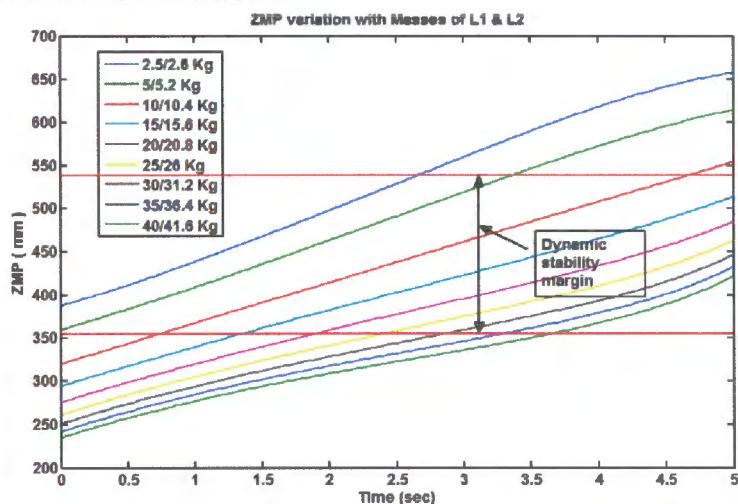
Figure 7.10 : Variation of ZMP with different values of L_1 and L_2

Figure (7.10) shows the ZMP variation with L_1 and L_2. According to this simulation result, it can be seen that the dynamic stability improves up to some limit of L_1 and L_2.

7.4 Application of simulation results

The above mentioned simulation results [7.3.1 to 7.3.6] are helpful in selecting proper parameters for the robot to maintain the dynamic stability. The parameters are, torso length, torso weight, step time and step length. The slope of the terrain can be measured.

With the aid of these parameters, another simulation can be performed to find out torso angle. This simulation will show the way to control the torso angle to maintain the dynamic stability. These values are compulsory for fabrication of the robot.
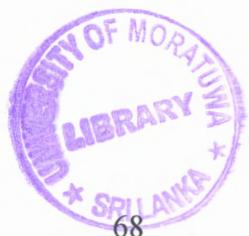
Chapter 8

Conclusion

8.1 Derived Kinematic model

Kinematics is the basic robotic theory that can be applied to model the bipedal walking. In this research study, a kinematic model is developed for ramp climbing bipedal robot by using Direct kinematic, Inverse kinematic, Link transformation matrix, Homogeneous transformation matrix and the DH notation

This is an effort to apply the basic robotics theories to solve real world problem. Also, this application is a direct approach rather than using indirect methods as artificial intelligence concepts.

Utilizing the above theory in chapter (3) the equations for joint angles of swing leg have been derived. That is the equations for thigh angle, knee angle, and ankle angle variation in swing leg.

In this formulation the swing leg was considered as planner manipulator and defined its base and end effector as hip and ankle respectively. The same equations for knee angle and ankle angle of stance leg have been derived in chapter (5), by utilizing the same theory but considering base and end effector as ankle and hip respectively.

But, there is a contradiction due to hip movement and to avoid this, another co-ordinate frame is introduced to hip and modify the swing leg kinematics to match with the moving base manipulator kinematics.

The assumption was made in derivation of stance leg kinematics as "The hip movement trajectory is a straight line parallel to the slope". In this chapter, an important invention is made regarding the hip movement, that is the hip movement distance is equal to half of the step length within one gait cycle. This is much similar to human walking. According to this concept it is needed to complete two gait cycle to move hip in one step length.

The correctness of the kinematic modeling have been checked by computer simulation. Before the simulation, the data file for thai angle, knee angle, ankle angle of swing leg and knee and ankle angles of stance leg was generated by using the set of equations obtained. Robo work simulation tool has been utilized since it supports dat. Files. By utilizing the above simulation results, the smoothness of the joint angle variation and level of accuracy of the derivation can be guaranteed.

The dynamic stability is checked in chapter (6) by calculating ZMP for lower body. Method for calculation of ZMP for bipedal robot was included in this chapter, and the steps of calculations are clearly shown. The dynamic stability for lower body is analyzed by

using mathlab software and the graph ZMP Vs time was plotted. Using the graph and the concept DBM, it is proved that the robot lower body is unstable. That means the position of ZMP is in unsafe zone. The methods for moving ZMP to safe zone are stated in chapter (7) and the best method is finalized as addition of torso and controlling the torso angle.

Future Work

1. In this research the proposed model contained only torso for upper body. As a research extension, addition of shoulders can be considered to analyze the dynamic stability.

2. this research only the kinematic model is developed. The dynamic model or Equation of Motion (EOM) calculations tend to derivation of joint torque equations. The control of bipedal walking can be implemented by CTC like control method as a future work in the fabrication stage.

3. The foot reaction force is not considered in this research. By considering the foot reaction force and friction force exerted by the terrain, the maximum inclination of the slope can be estimated. This is the maximum angle of inclination of the terrain that the robot can walk without slipping.

4. This model can be modified to investigate the walking pattern when altering the environment. As an example, modeling of "under water walking robot" being the latest idea.

5. The final equation is a very complex, nonlinear, second order differential equation.. To handle this problem two methods are proposed:

   i. Trial and error method

   We can check the ZMP using the above equation by substituting several torso angles at several time instants. If ZMP is not a safe margin at any instant the torso angle is needed to be changed to shift the ZMP to the safe region.

   ii. Using Artificial Intelligence Applications

   This type of problems can be handled by using Artificial Intelligence Techniques. For an example, as an extension of the research, the optimized torso angle can be obtained by using genetic algorithm by considering the ZMP equation as the objective function

70

References:

[1] Rolan Sigheward, Illah R.Nourbakhsh, "Introduction to Autonomous Mobile Robots," A text book of Robotic Technology, pp 1-19, 2005.

[2] Pandu Ranga Vundavilli, Dillip Kumar Prathihar, "Soft Computing-based Gait Planners for a Dynamically Balanced Biped Robot Negotiating Sloping Surfaces,"Applied Soft Computing Journal Paper, April 2008.

[3] Eirk V. Cuevas, Daniel Zaldivar, Raul Rojs, "Bipedal Robot Description," Technical Report, January 2005

[4] T. Kato, A. Takanishi, H. Jishikawa, and I. Kato, "The realization of the quasi-dynamic walking by the biped walking machine," in Fourth Symposium on Theory and Practice of Robots and Manipulators, pp. 341–351, Polish Scientific Publishers, 1983.

[5] A. Takanishi, M. Ishida, Y. Yamazaki, and I. Kato, "The realization of dynamic walking by the biped walking robot WL-10RD," in ICAR'85, pp. 459–466, 1985.

[6] H.Miura and I. Shimoyama, "Dynamicwalk of a Biped," International Journal of Robotics Research, vol. 3, pp. 60–74, 1984.

[7] M. H. Raibert, "Balanced Legged Robots," Cambridge, MA: MIT Press, 1986.

[8] J. Hodgins, J. Koechling, and M. H. Raibert, "Running experiments with a planar biped," in Robotics Research: the 3rd Int. Symposium, pp. 349–355, MIT Press, 1986.

[9] S. Kajita, T. Yamaura, and A. Kobayashi, "Dynamic walking control of a biped robot along a potential energy conserving orbit," IEEE Transactions on Robotics and Automation, pp. 431–438, Aug. 1992.

[10] A. Takanishi, H.-o. Lim, M. Tsuda, and I. Kato, "Realisation of dynamic biped walking stabilized by trunk motion on a sagitally uneven surface," in Proceedings of the 1990 IEEE Int. Workshop on Intelligent Robots and Systems (IROS), pp. 323–330, 1990.

[11] J.-i. Yamaguchi, A. Takanishi, and I. Kato, "Development of a biped walking robot compensating for three-axis moment by trunk motion," in Proceedings of the 1993 IEEE/RSJ Int. Conference on Intelligent Robots and Systems (IROS), pp. 561–566, July 1993.

[12] T. McGeer, "Passive dynamic walking," International Journal of Robotics Research, vol. 9, pp. 62–82, 1990.

[13] M. Garcia, A. Chatterjee, A. Ruina, and M. Coleman, "The simplest walking model: Stability, complexity, and scaling," to appear in ASME Journal of Biomechanical Engineering, 1998.

[14] P. I. Doerschuk, V. D. Nguyen, and A. L. Li, "Neural network control of a three-link leg," in Proceedings of the Int. Conference on Tools with Artificial Intelligence, pp. 278–281, 1995.

[15] P. I. Doerschuk, V. Nguyen, W. Simon, and F. Kwong, "Intelligent ballistic control of a jointed leg," in Proceedings of the 1996 IEEE Int. Joint Symposium on Intelligence and Systems, pp. 117–124, 1996.

[16] W. T. Miller III, "Real-time neural network control of a biped walking robot," IEEE Control Systems, pp. 41–48, Feb. 1994.

[17] A. Kun andW. T. Miller III, "Adaptive dynamic balance of a biped using neural networks," in Proceedings of the 1996 IEEE International Conference on Robotics and Automation, pp. 240–245, April 1996.

[18] R.K. Mittal, I.J.Nagrath, "Robotics and Control," A text book of Robotics Technology, pp. 01-186, 2003.

[19] Taesin Ha, Chong-Ho Choi, "An Effective Trajectory Generation Method for Bipedal Walking," Robotics and Automation Journal, June 2007

[20] P.L.Muench, J.Alexander, S.Hadley, S.Starkey, "Bipedal Walking," A Research Paper, February 2002.

[21] Miomir Vukobratovic, Branislav Borovac, Dragolgub Surdiloic, "Zero-Moment Point –Proper Interpretation," USC Neuroscience Journal Paper, pp 1-7, January 2004

[22] S.M. Welihinda, "Simulation and Behavioral Analysis of Biped Robots," Master Thesis University of Moratuwa Sri Lanka, December, 2009

[23] Stuart Russell, Peter Norvig, "Artificial Intelligence-A Modern Approach," A text book, 2007

[24] A. Agrawal and S.K. Agrawal, "An approach to identify joint motions for dynamically stable walking," ASME Trans. Mechanical Design, vol.128, pp.649-653,P,2006.

[25] M.Y. Zarrugh and C.W. Radcliffe," Computer generation of human gait kinematics," J.Biomec, vol.12, pp. 99-111.